



THE HONG KONG  
POLYTECHNIC UNIVERSITY

香港理工大學

Pao Yue-kong Library

包玉剛圖書館

---

## Copyright Undertaking

This thesis is protected by copyright, with all rights reserved.

**By reading and using the thesis, the reader understands and agrees to the following terms:**

1. The reader will abide by the rules and legal ordinances governing copyright regarding the use of the thesis.
2. The reader will use the thesis for the purpose of research or private study only and not for distribution or further reproduction or any other purpose.
3. The reader agrees to indemnify and hold the University harmless from and against any loss, damage, cost, liability or expenses arising from copyright infringement or unauthorized usage.

### IMPORTANT

If you have reasons to believe that any materials in this thesis are deemed not suitable to be distributed in this form, or a copyright owner having difficulty with the material being included in our database, please contact [lbsys@polyu.edu.hk](mailto:lbsys@polyu.edu.hk) providing details. The Library will look into your claim and consider taking remedial action upon receipt of the written requests.

IMMOBILIZATION-FREE ELECTROCHEMICAL  
DETECTION OF ISOTHERMAL PRIMER  
GENERATION-ROLLING CIRCLE AMPLIFICATION  
FOR SIMPLE AND SENSITIVE DNA ANALYSIS

LEE CHUN DEREK

M.PHIL

THE HONG KONG

POLYTECHNIC UNIVERSITY

2013

The Hong Kong Polytechnic University

Interdisciplinary Division of Biomedical Engineering

Immobilization-Free Electrochemical Detection of  
Isothermal Primer Generation–Rolling Circle  
Amplification for Simple and Sensitive DNA Analysis

by

LEE Chun Derek

A thesis submitted in partial fulfillment of the requirements for  
the degree of Master of Philosophy

August 2012

## **Certificate of Originality**

I hereby declare that this thesis is my own work and that, to the best of my knowledge and belief, it reproduces no material previously published or written, nor material that has been accepted for the award of any other degree or diploma, except where due acknowledgement has been made in the text.

\_\_\_\_\_ (Signed)

Mr. LEE Chun Derek (Name of Author)

## **Abstract**

Electrochemical deoxyribonucleic acid (DNA) sensors have been widely studied in recent decades. Their simplicity, portability, and low cost are conducive to point-of-care and on-site applications. Typically, an electrode surface is immobilized with a capture probe, to which a complementary target sequence is hybridized, giving rise to a change in the electrochemical readout. Undesirably, the immobilization process usually requires the use of functionalized probe and is time-consuming. Besides, the hybridization of the target to the electrode-bound probe is much less efficient than solution-phase hybridization due to steric hindrance. In view of these issues, there has been an increasing interest in immobilization-free approach. Recent attempts have been particularly devoted to its coupling with enzymatic DNA amplification so as to achieve high sensitivity. One major challenge is to keep the entire assay components and procedures simple. In this study, a new immobilization-free electrochemical detection scheme coupled with isothermal DNA amplification reaction (primer generation–rolling circle amplification, PG–RCA) was developed. A redox indicator (methylene blue (MB)) and indium tin oxide (ITO) electrode were utilized for simple DNA detection. In the absence of the target, MB can freely diffuse to the ITO electrode to effect charge transfer and be detected by differential pulse voltammetry (DPV). While in the presence of the target, PG–RCA at an operating temperature of 37 °C produces in an exponential manner single-stranded amplicons, which forms complex with MB through intercalative binding. The complex has a lower DPV current than the free MB as a result of slower

diffusion to and electrostatic repulsion with the electrode. Results show that MB is compatible with PG-RCA and RCA reaction. The amplification power of PG-RCA is stronger than RCA. The electrochemical and fluorescence results also show that this new DNA detection method is specific and sensitive (with a detection limit of 100 fM) with linear working range from 100 fM to 1 nM. Reproducible measurements can be performed by simple electrode washing step. With the simple instrumentation and assay protocol, this new immobilization-free electrochemical detection platform could allow DNA analysis to be performed in a decentralized setting.

## **Acknowledgments**

I am heartily thankful to my chief supervisor, Dr. Thomas Lee, for his patient guidance, advice, and encouragement throughout my study. I would like to express my gratitude to my co-supervisor, Prof. Shea Ping Yip, for his advice on DNA amplification techniques. I would like to thank Prof. I-Ming Hsing at The Hong Kong University of Science and Technology for providing some of the electrodes. I would also like to thank my colleagues in laboratory S106B, who offered great support to my experiments. Besides, I would like to take this opportunity to thank all others who helped or supported me in different aspects during my study. Last but not least, I would like to thank my family for their unconditional love, support, and understanding throughout my life.

# List of Publications

## Journal article

Lee, D.C., Yip, S.P. & Lee, T.M.H. Simple and Sensitive Electrochemical DNA Detection of Primer Generation–Rolling Circle Amplification. *Electroanalysis*, **in press** (2013).

## Conference

Lee, D.C., Yip, S.P. & Lee, T.M.H. Immobilization-Free Electrochemical Detection of Isothermal Exponential DNA Amplification. *The HKUST International Conference on Biomedical Engineering*, **Poster** (2013).

# Table of Contents

<b>Certificate of Originality .....</b>	<b>i</b>
<b>Abstract .....</b>	<b>ii</b>
<b>Acknowledgments .....</b>	<b>iv</b>
<b>List of Publications.....</b>	<b>v</b>
<b>Table of Contents .....</b>	<b>vi</b>
<b>List of Figures .....</b>	<b>X</b>
<b>List of Table .....</b>	<b>XV</b>
<b>List of Abbreviations.....</b>	<b>xvi</b>
<b>Introduction .....</b>	<b>1</b>
1.1. EC DNA Sensors .....	2
1.1.1. Immobilization-Based EC DNA Sensors .....	2
1.1.1.1. Probe Immobilization Method .....	7
1.1.1.2. Probe Density .....	8
1.1.1.3. Electrode Surface Passivation .....	9
1.1.2. Immobilization-Free EC DNA Sensors .....	10
1.2. EC DNA Sensors with Enzymatic Target Sequence Amplification .....	12

1.2.1. PCR.....	13
1.2.2. EC DNA Sensors with PCR .....	14
1.2.2.1. Immobilization-Based EC DNA Sensors with PCR.....	15
1.2.2.2. Immobilization-Free EC DNA Sensors with PCR.....	18
1.2.3. Isothermal Amplification.....	24
1.2.4. EC DNA Sensors with Isothermal Amplification .....	30
1.2.4.1. Immobilization-Based EC DNA Sensors with Isothermal Amplification .....	30
1.2.4.2. Immobilization-Free EC DNA Sensors with Isothermal Amplification.	32
1.3. Current Limitations .....	36
1.4. Objectives of the Study .....	36
<b>Methodology .....</b>	<b>38</b>
2.1. Detection Scheme.....	38
2.1.1. Immobilization-Free EC DNA Detection Scheme .....	38
2.1.2. Immobilization-Free EC DNA Detection Scheme Combined with PG–RCA .....	40
2.1.3. PG–RCA with Molecular Beacon .....	42
2.2. Materials and Instrumentation.....	43
2.2.1. Reagents.....	43

2.2.2. Oligonucleotide Sequences.....	44
2.2.3. Instrumentation.....	45
2.2.4. Electrode Chips.....	45
2.3. Experimental Protocols .....	47
2.3.1. Circular Template Preparation.....	47
2.3.2. EC Measurement of MB with ssDNA.....	48
2.3.3. Real-Time Fluorescence Measurement of PG–RCA.....	48
2.3.4. Effect of MB on PG–RCA.....	49
2.3.5. EC Measurements of PG–RCA .....	49
2.3.6. Specificity Test .....	50
2.3.7. Sensitivity Test .....	50
2.3.8. Effect of BSA on EC Measurement.....	50
2.3.9. Regeneration of the ITO Electrode.....	50
2.3.10. EC Detection of PG–RCA at Different Time Points.....	51
2.3.11. PG–RCA Utilizing Beacon.....	51
<b>Results and Discussion.....</b>	<b>52</b>
3.1. EC Detection with Different Electrodes.....	52
3.2. Effect of MB Concentration on EC ssDNA Detection.....	54

3.3. Real-Time Fluorescence Measurement of PG–RCA .....	55
3.4. Effect of MB on PG–RCA .....	57
3.5. EC Measurements of PG–RCA .....	58
3.6. Specificity Test .....	59
3.7. Sensitivity Test .....	60
3.8. Absorption on ITO Electrode .....	62
3.9. Regeneration of ITO Electrode Surface .....	63
3.10. EC Detection of PG–RCA at Different Time Points .....	65
3.11. PG–RCA using DNA Beacon .....	66
<b>Conclusions and Recommendations for Future Work.....</b>	<b>68</b>
4.1. Key Findings and Conclusions .....	68
4.2. Recommendations for Future Work .....	69
<b>References .....</b>	<b>71</b>

## List of Figures

<b>Figure 1.1.</b> Scientific publications on electrochemistry of nucleic acids between 1958 and 2010 (Adapted from [8]). .....	<b>3</b>
<b>Figure 1.2.</b> Schematic illustration of the interaction (left) between RuHex and probe-immobilized electrode (Modified from [14]), as well as (right) between RuHex (purple), DM (red), MB (blue) and hybrid-immobilized electrode (Modified from [13]). .....	<b>4</b>
<b>Figure 1.3.</b> EC DNA detection using signaling probe with covalently-linked redox marker (Adapted from [15])......	<b>5</b>
<b>Figure 1.4.</b> EC detection of DNA by Fc-labeled beacon immobilized on gold electrode (Adapted from [16]). .....	<b>6</b>
<b>Figure 1.5.</b> Effect of probe density on EC signals in folding-based EC DNA detection scheme with covalently-linked redox marker (Adapted from [39])......	<b>10</b>
<b>Figure 1.6.</b> MCH treatment on the probe-immobilized surface (Adapted from [41]). ..	<b>11</b>
<b>Figure 1.7.</b> Immobilization-free EC DNA detection using Fc-PNA probe (Adapted from [44])......	<b>12</b>
<b>Figure 1.8.</b> Schematic illustration of the thermal cycling process of PCR (Modified from [4])......	<b>14</b>
<b>Figure 1.9.</b> Microdevice for PCR DNA amplification and end-point EC detection (Adapted from [36]). (A) Analyte with PCR-mix is applied into the reaction chamber; (B) Asymmetric PCR is performed to generate adequate amplicons; (C) Hybridization	

of the amplicons to the immobilized probe on the electrode surface; (D) Binding of redox indicator for EC signal transduction. ....	16
<b>Figure 1.10.</b> Fully integrated biochip for sample preparation, PCR amplification, and EC detection (Adapted from [48]). ....	17
<b>Figure 1.11.</b> Microdevice for simultaneous PCR DNA amplification and real-time monitoring (Adapted from [50]). ....	18
<b>Figure 1.12.</b> Immobilization-free EC detection of PCR amplicons using Hoechst 33258 (Adapted from [51]). (A) Freely moving Hoechst 33258 favors EC transduction; (B) Binding of Hoechst 33258 to DNA inhibits the EC transduction; (C) EC signal suppressed by target DNA. ....	19
<b>Figure 1.13.</b> (Top) Layout of the integrated continuous-flow PCR and EC detection microchip and (bottom) EC detection scheme utilizing MB as redox indicator (Adapted from [52]). ....	21
<b>Figure 1.14.</b> (Top, a–c) Layout of the custom-made EC cells for real-time PCR monitoring and (bottom) EC detection scheme based on catalytic oxidation of dGTP or 7-deaza-dGTP (Modified from [53]). ....	22
<b>Figure 1.15.</b> Schematic illustration of real-time immobilization-free EC detection scheme based on redox intercalator of $\text{Os}[(\text{bpy})_2\text{DPPZ}]^{2+}$ (Adapted from [54]). ....	23
<b>Figure 1.16.</b> Immobilization-free EC detection scheme using eTaq probe (Adapted from [55]). ....	24
<b>Figure 1.17.</b> Schematic illustration of RCA (Modified from [58]). ....	26
<b>Figure 1.18.</b> Schematic illustration of LAMP (Adapted from [59]). ....	27

<b>Figure 1.19.</b> Schematic illustration of isothermal circular strand displacement polymerization reaction (Adapted from [61]). .....	<b>28</b>
<b>Figure 1.20.</b> Schematic illustration of PG–RCA (Adapted from [62]). .....	<b>29</b>
<b>Figure 1.21.</b> Immobilization-based EC detection of viral DNA with RCA using Fc-dUTP redox marker and enzymatic signal amplification (Adapted from [76]). .....	<b>30</b>
<b>Figure 1.22.</b> Immobilization-based EC DNA detection with ligation and RCA using MB redox indicator (Adapted from [75]). (A) Schematic illustration for SNP detection; (B) Hybridization of RCA amplicons to immobilized probe for EC signal detection. ....	<b>31</b>
<b>Figure 1.23.</b> Immobilization-free EC DNA sensor with LAMP utilizing Hoechst 33258 (Adapted from [79]). .....	<b>33</b>
<b>Figure 1.24.</b> Immobilization-free EC DNA sensor with strand-displacement polymerization reaction using Fc-PNA probe (Adapted from [81]). .....	<b>35</b>
<b>Figure 1.25.</b> Immobilization-free EC DNA sensor with LAMP using MB redox indicator (Adapted from [82]). .....	<b>35</b>
<b>Figure 2.1.</b> Immobilization-free EC DNA detection scheme using MB. ....	<b>39</b>
<b>Figure 2.2.</b> Schematic illustration of DPV waveform. (A) Linear staircase wave; (B) Regular pulse wave; (C) Differential pulse wave. ....	<b>40</b>
<b>Figure 2.3.</b> The immobilization-free EC detection scheme combined with PG–RCA. .	<b>41</b>
<b>Figure 2.4.</b> Schematic illustration of molecular beacon as target recognition probe as well as primer for PG–RCA reaction. The target sequence is marked in blue. ....	<b>42</b>
<b>Figure 2.5.</b> Schematic illustration of the PDMS-bonded electrode chip. ....	<b>47</b>

<b>Figure 3.1.</b> DPV measurements of MB without and with ssDNA using gold working electrode. ....	<b>53</b>
<b>Figure 3.2.</b> DPV measurements of MB without and with ssDNA using Pt working electrode. ....	<b>53</b>
<b>Figure 3.3.</b> DPV measurements of MB without and with ssDNA using ITO working electrode. ....	<b>54</b>
<b>Figure 3.4.</b> DPV peak current difference between free MB and ssDNA-bound MB as a function of MB concentration on ITO electrode. ....	<b>55</b>
<b>Figure 3.5.</b> Real-time fluorescence measurement results of PG-RCA and RCA in the presence of 1 nM analyte; and control (without analyte). ....	<b>56</b>
<b>Figure 3.6.</b> Agarose gel electrophoresis results showing the effects of MB on PG-RCA and RCA. Lane L: DNA ladder; lanes 1, 3, 5, and 7: without MB; lanes 2, 4, 6, and 8: with 20 $\mu$ M MB; lanes 5 and 6: RCA with 10 nM analyte; lanes 7 and 8: PG-RCA with 1 nM analyte; lanes 1–4: control reactions (without analyte) for lanes 5–8. ....	<b>57</b>
<b>Figure 3.7.</b> EC detection results of PG-RCA and RCA in the presence of 1 nM analyte; and control (without analyte). ....	<b>58</b>
<b>Figure 3.8.</b> Real-time fluorescence measurement results of PG-RCA with the analyte, non-complementary sequence (non-comp), and control (no analyte). ....	<b>59</b>
<b>Figure 3.9.</b> EC detection results of PG-RCA with the analyte, non-complementary sequence (non-comp), and control (no analyte). ....	<b>60</b>
<b>Figure 3.10.</b> Real-time fluorescence measurement results of PG-RCA with different concentrations of analyte. ....	<b>61</b>

<b>Figure 3.11.</b> EC detection results of PG–RCA with different concentrations of analyte. .....	<b>61</b>
<b>Figure 3.12.</b> Plot of peak current against logarithm of analyte concentration with constant MB concentration. ....	<b>62</b>
<b>Figure 3.13.</b> EC measurements of MB in solution containing BSA at different time points. ....	<b>63</b>
<b>Figure 3.14.</b> Regeneration of ITO electrode surface by water rinsing. ....	<b>64</b>
<b>Figure 3.15.</b> Regeneration of ITO electrode surface by sonication in water. ....	<b>64</b>
<b>Figure 3.16.</b> Plot of DPV signal change as a function of PG–RCA reaction time.....	<b>65</b>
<b>Figure 3.17.</b> Real-time fluorescence measurement results of PG–RCA utilizing beacon. .....	<b>66</b>
<b>Figure 3.18.</b> EC measurement results of PG–RCA utilizing beacon. ....	<b>67</b>

## List of Table

<b>Table 2.1.</b> Oligonucleotide sequences used in this study .....	<b>44</b>
--	-----------

## List of Abbreviations

A	adenine
Ag/AgCl	silver/silver chloride
Bp	base pair
BSA	bovine serum albumin
C	cytosine
Co(bpy) <sub>3</sub> <sup>3+</sup>	tris(2,2'-bipyridyl)cobalt(III)
Co(phen) <sub>3</sub> <sup>3+</sup>	tris(1,10-phenanthroline)cobalt(III)
dGTP	2'-deoxyguanosine 5'-triphosphate
dNTPs	deoxynucleoside triphosphates
dsDNA	double-stranded DNA
DM	daunomycin
DNA	deoxyribonucleic acid
DPV	differential pulse voltammetry
DTT	dithiothreitol
EC	electrochemical
ECP	electroconducting polymer
Fc	ferrocene
Fc-dUTP	ferrocene-labeled deoxyuridine triphosphate
Fc-PNA	ferrocene-labeled peptide nucleic acid
G	guanine

ITO	indium tin oxide
LAMP	loop-mediated isothermal amplification
MB	methylene blue
MCH	mercaptohexanol
PCR	polymerase chain reaction
PDMS	polydimethylsiloxane
PG-RCA	primer generation-rolling circle amplification
PNA	peptide nucleic acid
Pt	platinum
RB	reaction buffer
RCA	rolling circle amplification
RuHex	hexaammineruthenium
ssDNA	single-stranded DNA
SAM	self-assembled monolayer
SNP	single-nucleotide polymorphism
T	thymine
TCEP	tris(2-carboxyethyl)phosphine

# **Chapter 1**

## **Introduction**

Deoxyribonucleic acid (DNA) detection plays an important role in diseases diagnosis. The early and accurate detection of viruses, bacteria, cancer cells or genetic diseases can facilitate physicians to prescribe prompt and effective treatment for patients. Over the past few decades, fluorescence-based techniques, which feature high sensitivity, have been widely used for DNA detection [1-4]. Nevertheless, fluorescence detection systems require bulky and sophisticated optical instrument, limiting their use in clinical laboratories. Electrochemical (EC) DNA sensors, on the other hand, have received increasing attention for point-of-care and on-site diagnostic applications thanks to their advantages of simplicity, portability, and low cost [5-8]. In recent years, the coupling of EC DNA sensor with enzymatic amplification of target sequence has dramatically increased the assay sensitivity [5]. Background information of EC DNA sensors is given in Section 1.1. A literature review of EC DNA sensors coupled with enzymatic target sequence amplification is presented in Section 1.2. The limitations of the current approaches and the objectives of this study are described in Section 1.3 and Section 1.4, respectively.

## **1.1. EC DNA Sensors**

EC DNA sensors can be broadly defined as devices that couple a DNA recognition element with an EC transducer. Specifically, the hybridization of a specific DNA sequence with the DNA recognition element (termed as probe) is converted into a useful EC signal. The field of EC DNA sensors originates from the EC studies of DNA. Between 1958 and 1993, the main focuses were direct electrochemistry of DNA and study of redox-active/electroactive species bound to DNA [8]. The number of research papers on the electrochemistry of nucleic acids has grown dramatically since early 1990s (Figure 1.1). One reason is the first demonstration of sequence-specific EC DNA detection by Millan and Mikkelsen in 1993 [9]. Numerous EC DNA sensors have been developed over the past two decades, which can be grouped into two categories: immobilization-based and immobilization-free approaches. The former one involves the attachment/binding of a probe onto an electrode surface while the latter one features the hybridization between probe and target sequence in the solution phase. Details of the two approaches are described in the following sections.

### **1.1.1. Immobilization-Based EC DNA Sensors**

The first EC DNA sensor developed by Millan and Mikkelsen was based on the immobilization approach [9]. Oligonucleotide probe with deoxyguanosine residues was covalently immobilized onto glassy carbon electrode. This immobilized probe hybridized with a complementary target sequence based on Watson–Crick base pairing

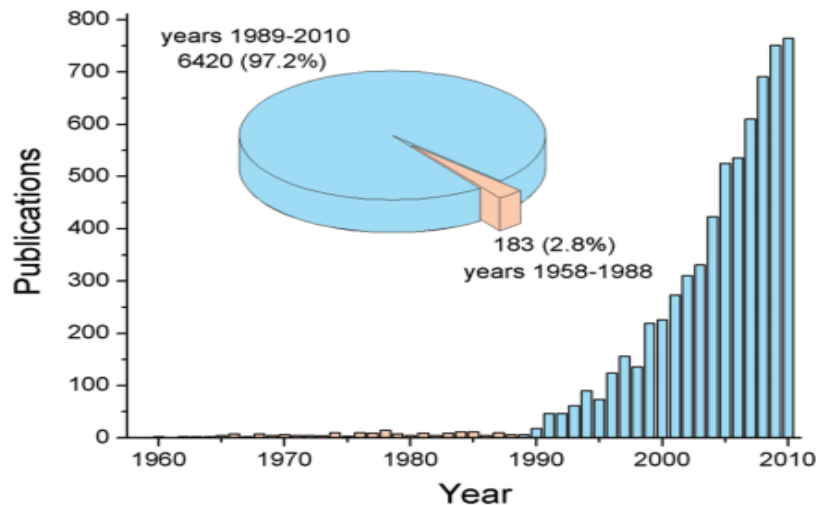


**Figure 1.1.** Scientific publications on electrochemistry of nucleic acids between 1958 and 2010 (Adapted from [8]).

(adenine (A) with thymine (T) and guanine (G) with cytosine (C)) [10]. The hybridization event was indicated by electroactive intercalator of tris(2,2'-bipyridyl)cobalt(III) ( $\text{Co}(\text{bpy})_3^{3+}$ ) or tris(1,10-phenanthroline)cobalt(III) ( $\text{Co}(\text{phen})_3^{3+}$ ) that bound preferentially to double-stranded DNA (dsDNA) than to single-stranded DNA (ssDNA). Therefore, in the presence of the target sequence, the EC signal (voltammetric peak current) from the bound electroactive intercalator increased.

Various immobilization-based EC DNA sensors have been devised with different signal transduction mechanisms including label-based and label-free approaches. Analogous to  $\text{Co}(\text{bpy})_3^{3+}$  and  $\text{Co}(\text{phen})_3^{3+}$ , other electroactive intercalator have also be used. For example, Hashimito and co-workers successfully utilized Hoechst 33258 (a DNA minor

groove binder) to differentiate between probe-modified and hybrid-formed gold electrode [11]. Tarlov and co-workers made use of hexaammineruthenium (RuHex) as a hybridization indicator [12]. RuHex is positively charged and would bind to the negatively charged sugar-phosphate backbone of DNA by electrostatic interaction (Figure 1.2). With a complementary target sequence hybridized to an electrode-bound probe, more RuHex molecules were brought close to the electrode surface, which were quantified by chronocoulometry. Barton and co-workers demonstrated that perfectly matched dsDNA-immobilized gold electrode could be easily distinguished from single-base mismatched one using intercalator of daunomycin (DM) and methylene blue (MB) (Figure 1.2) [13].

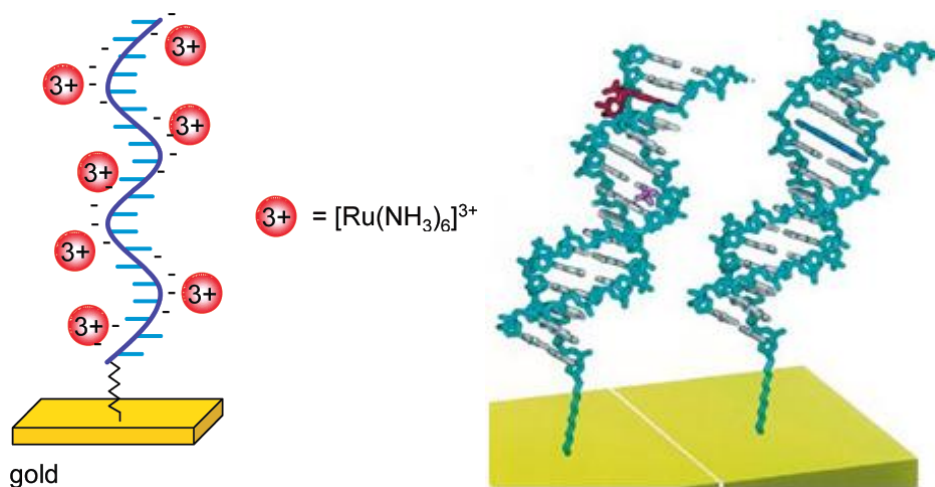


**Figure 1.2.** Schematic illustration of the interaction (left) between RuHex and probe-immobilized electrode (Modified from [14]), as well as (right) between RuHex (purple), DM (red), MB (blue) and hybrid-immobilized electrode (Modified from [13]).

Oligonucleotide probes with covalently-linked redox markers have also been used for immobilization-based EC DNA sensors. Farkas and co-workers reported a novel platform that allowed wash-free detection (the intercalator-based approaches mentioned above required removal of unbound sequences and intercalators before the EC measurements) [15]. A gold electrode was functionalized with a mixed self-assembled monolayer (SAM) of capture probe, polyglycol insulator, and phenylacetylene molecular wire. Upon the hybridization of a target sequence to the capture probe, a signaling probe with covalently-linked ferrocene (Fc) redox marker was brought into contact with the molecular wire, allowing charge transfer with the electrode (Figure 1.3).

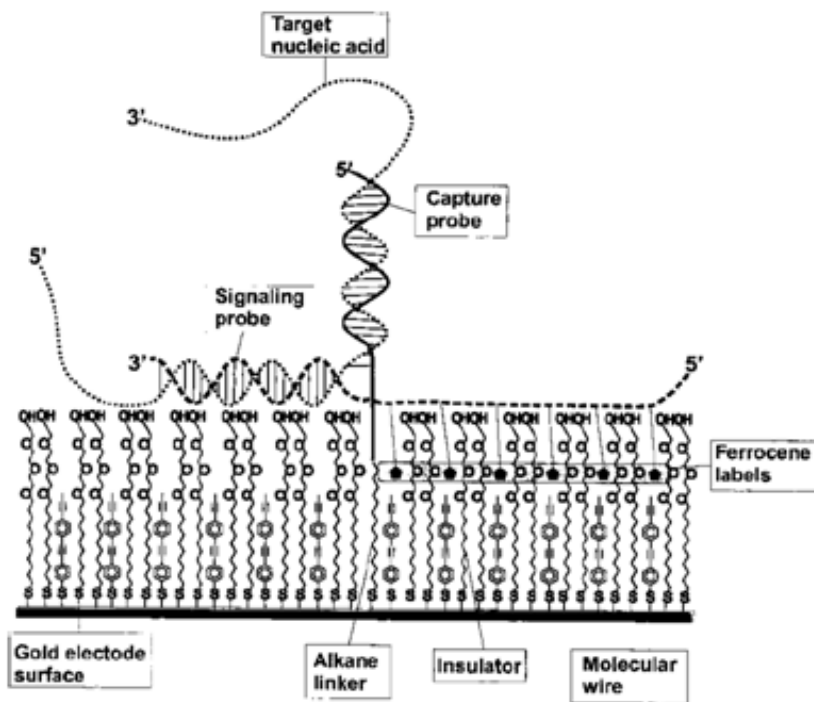


**Figure 1.3.** EC DNA detection using signaling probe with covalently-linked redox marker (Adapted from [15]).

Another novel platform was developed by Plaxco and co-workers based on a beacon-type capture probe with covalently-linked Fc redox marker [16]. As shown in Figure 1.4, in the absence of a complementary target sequence, the beacon adopted a stem-loop/folded structure, which brought Fc close to an electrode surface and thus charge transfer was facilitated. Upon the hybridization of the target, unfolding of the probe moved Fc away from the electrode surface and hence charge transfer was suppressed. It should be noted that other redox markers such as MB can also be used [17-18]. One attractive feature of this sensor was the capability of detecting the target in real sample matrix such as blood serum [18].

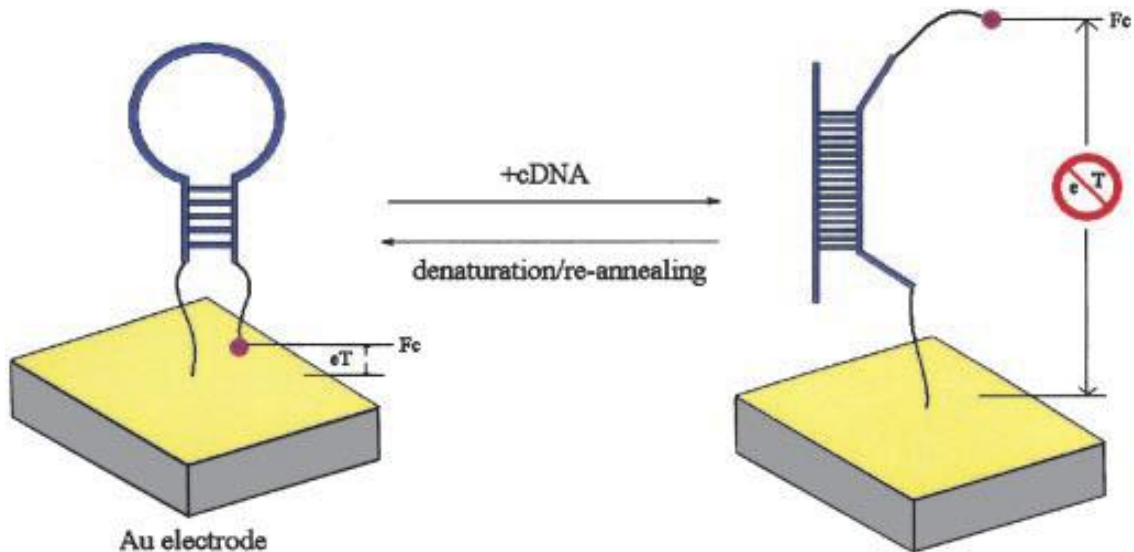


**Figure 1.4.** EC detection of DNA by Fc-labeled beacon immobilized on gold electrode (Adapted from [16]).

Enzyme [19-20] and nanoparticle [21-23] labels have also been utilized for immobilization-based EC DNA sensors. Alternatively, label-free approaches that rely on the intrinsic electroactivity of DNA bases (in particular G base) [24-25] as well as change in charge transfer property of electroconducting polymer (ECP)-based [26] or field effect transistor-based [27-28] sensors due to the hybridization event. It is important to emphasize that the performance of the immobilization-based EC DNA sensors depends on several crucial parameters including probe immobilization method, probe density, and electrode surface passivation, as discussed in detail below.

#### **1.1.1.1. Probe Immobilization Method**

In all previous examples, the capture probes were end-attached to the electrodes so that the DNA backbones of the recognition sequences were oriented toward the aqueous environment. This configuration, rather than lying on the electrode surface by adsorption, ensures all bases of the recognition sequence be accessible for hybridization. The choice of immobilization chemistry is largely dependent on the electrode material (e.g., gold, carbon, and indium tin oxide (ITO)). For gold electrode, chemisorption with gold–thiol linkage has been most widely employed with the use of thiolated DNA [29]. Prior to the immobilization, a deprotection step is needed to cleave the disulfide bond of the thiolated DNA. This is commonly carried out with reducing agent of dithiothreitol (DTT) [30-31] or tris(2-carboxyethyl)phosphine (TCEP) [31], followed by the purification of the activated DNA from the reducing agent using chromatographic technique. For carbon electrode, immobilization via end-attachment is not

straightforward. In the work by Millan and Mikkelsen mentioned earlier [9], glassy carbon electrode was first oxidized in 2.5% potassium dichromate and 10% nitric acid at an applied voltage of +1.5 V for 15 s. Then, a deoxyguanosine-functionalized probe was covalently attached to the oxidized carbon by means of carbodiimide chemistry. Another end-attachment method was reported by Marrazza and Mascini [32]. Avidin was first adsorbed onto screen-printed graphite electrode, to which a biotin-functionalized probe was attached. For ITO electrode, additional linker molecules with functional groups of carboxylate [33-34], phosphonate [35], and trialkoxysilane [36] were needed. Capture probes were then attached to the linkers by covalent bonds. Alternatively, ECP could be used for direct (ECP-functionalized probe) or two-step (electropolymerization followed by covalent probe attachment) probe immobilization [37-38].

#### **1.1.1.2. Probe Density**

Probe density also plays a crucial role in the performance of the immobilization-based DNA sensors. Tarlov and co-workers studied the effect of probe density on hybridization efficiency [12]. They found that the hybridization efficiency would not increase linearly with increasing probe density. The main reason was due to the steric hindrance effect on the surface. The crowding of negatively charged probe surface hindered the hybridization of target molecules due to the great charge repulsion. The optimum probe density in their work was found to be  $4 \times 10^{12}$  molecules/cm<sup>2</sup>.

Apart from hybridization efficiency, Plaxco and co-workers showed that probe density had a significant effect on the EC signals [16,39-40]. With a beacon-type capture probe covalently-labeled with a redox marker, the no-target current (i.e., without a complementary target sequence that the redox marker was in close proximity with an electrode surface) for the case of high probe density was, as expected, higher than that of medium probe density. Upon the hybridization of the target, there was a 50% decrease in the peak current for the high probe density one while 15% for the medium one (Figure 1.5). As mentioned earlier, in fact for the high probe density sensor, the unfolding of the probe moved the redox marker away from the electrode surface and hence charge transfer was significantly suppressed. The smaller current change for the medium probe density sensor was attributed to the possible bending of the rigid hybrid structure toward the electrode surface and thus charge transfer was less suppressed. The optimum probe density for this sensor was  $2.1 \times 10^{12}$  molecules/cm<sup>2</sup>.

### **1.1.1.3. Electrode Surface Passivation**

Surface passivation is yet another important factor influencing the performance of the immobilization-based DNA sensors, especially specificity. Take gold electrode as an example, during the immobilization of a thiolated oligonucleotide, besides the gold–thiol linkage, non-specific interaction between DNA bases and gold occurs, making the immobilized strand lying on the surface. Herne and Tarlov pioneered the use of mercaptohexanol (MCH) to remove such non-specific interaction [12], since the mercapto group of MCH has higher affinity than the non-specific interaction of DNA

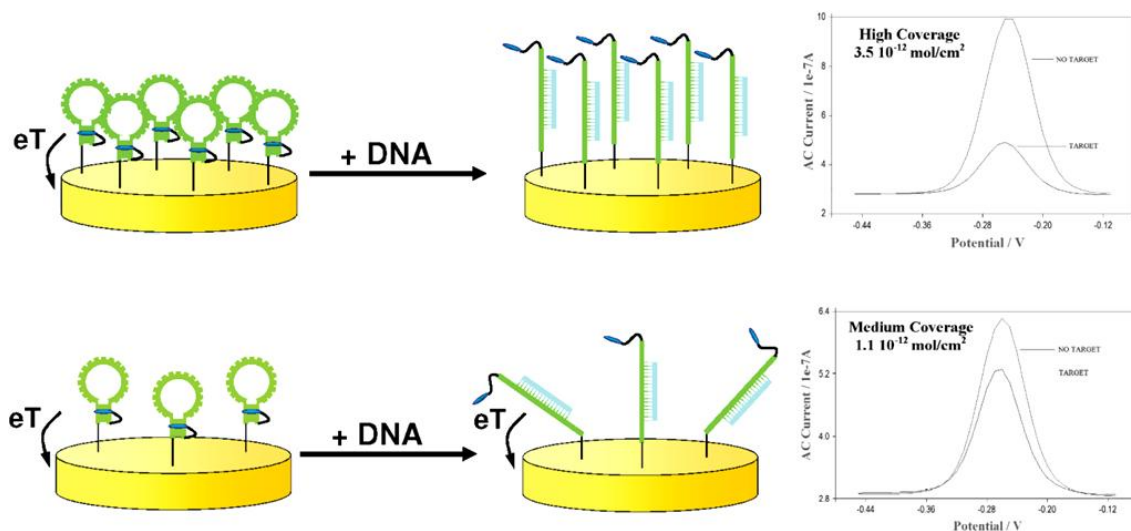


**Figure 1.5.** Effect of probe density on EC signals in folding-based EC DNA detection scheme with covalently-linked redox marker (Adapted from [39]).

bases (amine groups) with gold. As a consequence, the adsorbed bases were displaced and the immobilized strand was oriented toward the aqueous environment (Figure 1.6) [41]. The resulting mixed SAM, densely filled with MCH having hydroxyl groups exposed to the aqueous environment, could effectively minimize non-specific adsorption of non-complementary sequences to the surface [8,12,16,41-42].

### 1.1.2. Immobilization-Free EC DNA Sensors

The immobilization and passivation steps as well as the hybridization process on electrode surface are time-consuming, which normally take more than 10 hours in total [12,16-17,41]. Moreover, the use of modified oligonucleotides for immobilization incurs extra cost. In 2004, Tamiya and co-workers demonstrated the first immobilization-free

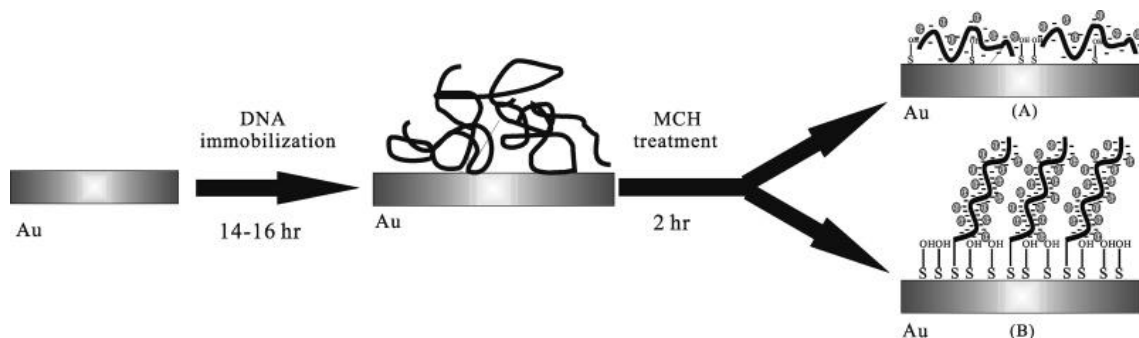


**Figure 1.6.** MCH treatment on the probe-immobilized surface (Adapted from [41]).

EC scheme for sequence-specific DNA detection that addressed the above issues [43]. Details of the scheme are presented in Section 1.2.2.2 as it involved enzymatic target sequence amplification.

In 2007, Hsing and co-workers developed another immobilization-free EC DNA detection scheme (without target sequence amplification) by using an Fc-labeled peptide nucleic acid (Fc-PNA) probe [44]. Peptide nucleic acid (PNA) is a DNA analog with the negatively charged sugar-phosphate backbone replaced by a neutral pseudo-peptide backbone (N-(2-aminoethyl)glycine units linked by peptide bonds) [45]. The Fc-PNA probe could freely make contact with an ITO electrode surface (even though negatively charged) and an anodic current peak was observed when monitored by differential pulse voltammetry (DPV). Upon the hybridization of a complementary target sequence to the Fc-PNA probe, the hybrid, which was negatively charged, was prohibited from approaching the ITO electrode surface due to electrostatic repulsion and thus the anodic current peak was suppressed (Figure 1.7).

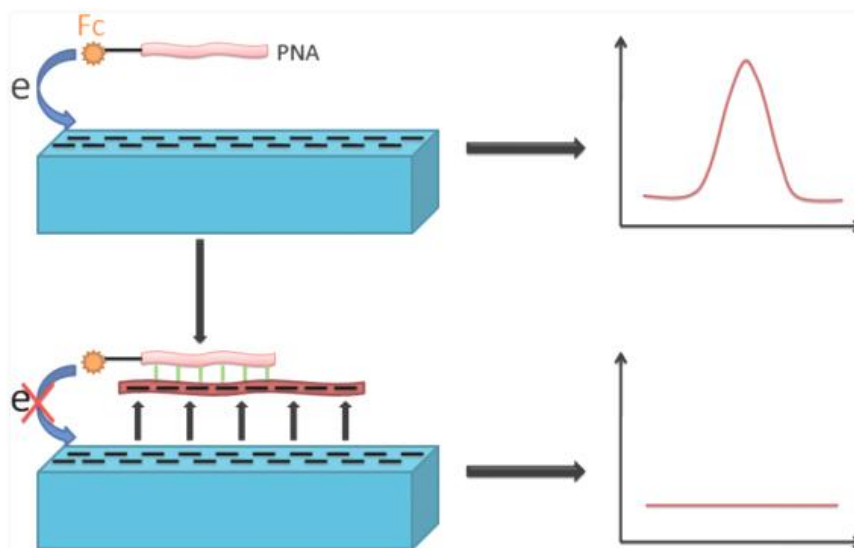


**Figure 1.7.** Immobilization-free EC DNA detection using Fc-PNA probe (Adapted from [44]).

## 1.2. EC DNA Sensors with Enzymatic Target Sequence Amplification

It is always desirable to achieve high detection sensitivity. Two strategies can be employed to accomplish this goal: signal amplification and target sequence amplification. Examples of the signal amplification strategy include enzyme [19-20] and nanoparticle [21-23] labels used in the immobilization-based sensors. For target sequence amplification, thermal cycling (polymerase chain reaction, PCR) and isothermal reactions, which have been routinely practiced in clinical and research laboratories with superior amplification power, are receiving increasing attention to be coupled with EC DNA sensors. A brief introduction of the different enzymatic target

sequence amplification schemes and their integration with EC detection platforms are given in the following sections.

### **1.2.1. PCR**

PCR was invented by Mullis and co-workers [46], which has become one of the most widely used techniques in molecular biology. It is an exponential DNA amplification technique by means of a thermal cycling process. Key PCR reaction components include a pair of primers (oligonucleotides that define the target sequence to be amplified), deoxyribonucleoside triphosphates (dNTPs), and thermostable DNA polymerase. As shown in Figure 1.8, the first step in PCR is denaturation. At 94 °C, typically for a duration of about 30 s, dsDNA template is heat dissociated into ssDNA constituents. Then, the temperature is cooled to 60 °C for primer annealing (i.e., hybridization of the primers to the target sequence). This is followed by extension of the hybridized primers through dNTPs incorporation based on Watson–Crick base pairing. The temperature of the extension step is dependent on the DNA polymerase used. For Taq DNA polymerase, the optimum temperature is 72 °C. The extension time is determined by the processivity of the DNA polymerase (Taq DNA polymerase can incorporate 1,000 bases in 1 min). After one thermal cycle, the amount of the target sequence is doubled. Hence, for a 30-cycle PCR, a single copy of the target DNA sequence is amplified to one billion copies. Currently, PCR product quantification methods in clinical laboratories are mainly based

on real-time fluorescence measurements [4] using SYBR Green I [47], molecular beacon [2], and TaqMan probe [3].

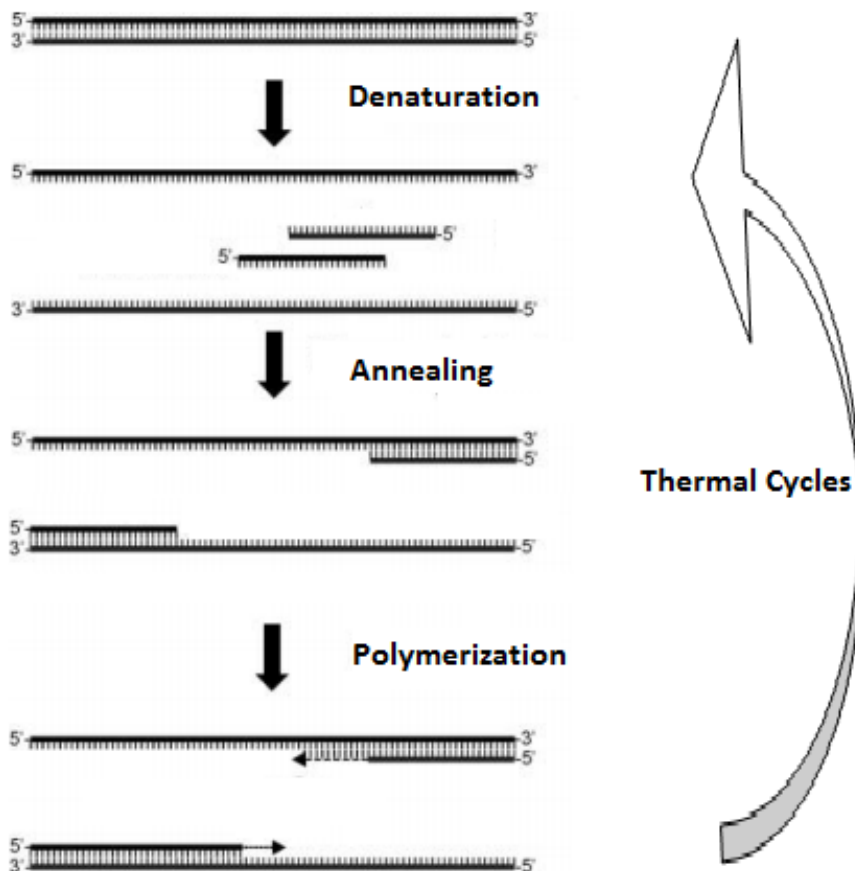


**Figure 1.8.** Schematic illustration of the thermal cycling process of PCR (Modified from [4]).

### 1.2.2. EC DNA Sensors with PCR

There have been many EC DNA sensors that were utilized for the detection of PCR amplicons, as reviewed by Luo and Hsing [5]. In this section, immobilization-based

sensors with PCR and EC detection integrated on microfabricated devices are first presented. Then, immobilization-free sensors for end-point and real-time PCR product detection are presented.

#### **1.2.2.1. Immobilization-Based EC DNA Sensors with PCR**

In 2003, Hsing and co-workers first reported an integrated microchip for PCR and end-point EC detection of PCR amplicons (Figure 1.9) [36]. A PCR reaction chamber was fabricated on a silicon microchip with integrated heaters and temperature sensors for rapid thermal cycling. The reaction chamber was sealed with a glass substrate, which also comprised patterned electrodes (gold working electrode as well as platinum (Pt) counter and pseudo-reference electrodes) for EC detection. The gold electrode had a capture probe immobilized via gold–thiol linkage. In the presence of a target DNA, asymmetric PCR generated single-stranded rich PCR amplicons. After the amplification reaction, the electrode-bound capture probe hybridized with the single-stranded PCR amplicons. A washing step was carried out to remove any unhybridized amplicons. Then, a redox intercalator (Hoechst 32258) was introduced into the reaction chamber. More intercalator molecules bound to the capture probe–amplicon hybrid than to the capture probe alone, thereby resulting in a higher anodic current peak during DPV measurements.

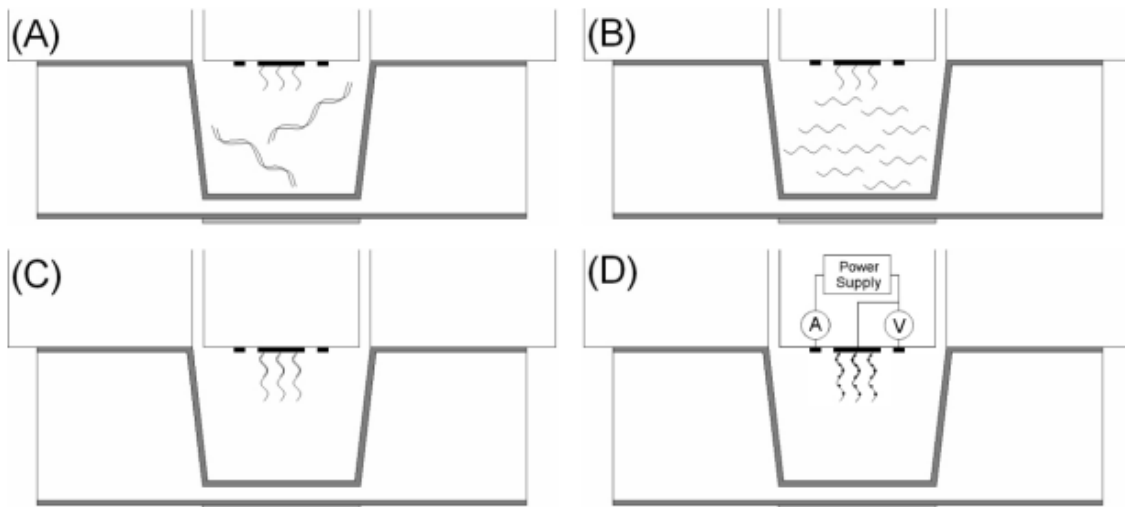


**Figure 1.9.** Microdevice for PCR DNA amplification and end-point EC detection (Adapted from [36]). (A) Analyte with PCR-mix is applied into the reaction chamber; (B) Asymmetric PCR is performed to generate adequate amplicons; (C) Hybridization of the amplicons to the immobilized probe on the electrode surface; (D) Binding of redox indicator for EC signal transduction.

In 2004, Liu and co-workers developed a self-contained and fully integrated biochip to perform DNA analysis of complex biological sample solutions (Figure 1.10) [48]. This biochip consisted of sample preparation, DNA amplification, and EC DNA detection units. On-chip pumps and valves were included for fluidic control. The assay commenced with the isolation of *E. coli* K12 cells from whole blood samples using immunomagnetic beads. This was followed by thermal lysis of the isolated cells and asymmetric PCR amplification of an *E. coli* K12-specific sequence. Subsequently, the single-stranded rich PCR amplicons were electrochemically detected by a gold electrode

functionalized with a mixed SAM of capture probe, polyglycol insulator, and phenylacetylene molecular wire, as detailed in Section 1.1.1.

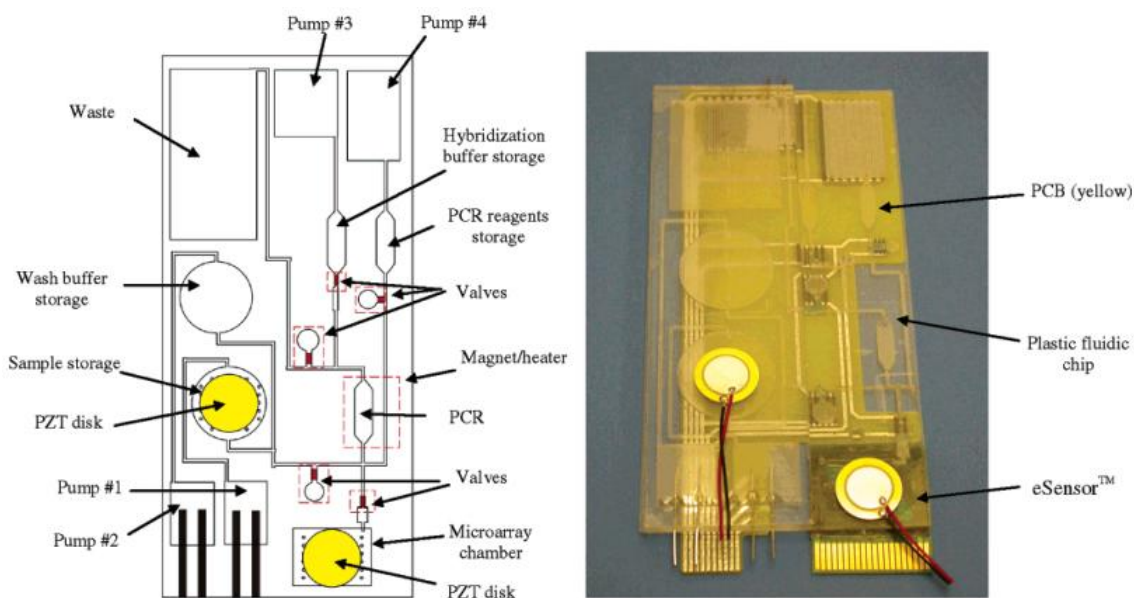


**Figure 1.10.** Fully integrated biochip for sample preparation, PCR amplification, and EC detection (Adapted from [48]).

Hsing and co-workers reported another integrated microchip for PCR and real-time EC detection of PCR amplicons (Figure 1.11) [49-50]. A silicon-glass microchip with EC detection electrodes (ITO working electrode as well as Pt counter and pseudo-reference electrodes) was employed. The ITO working electrode surface was covalently functionalized with a capture probe via a trialkoxysilane linker. PCR was performed with 30% of deoxythymidine triphosphate substituted by Fc-labeled deoxyuridine triphosphate (Fc-dUTP). In the presence of a target sequence, PCR amplicons were

generated. The capture probe when hybridized with the amplicons was extended and thus Fc-dUTP was incorporated. The accumulation of Fc close to the electrode surface produced an anodic current peak in DPV measurement. Cycle-by-cycle EC measurement was possible, enabling real-time monitoring of the amplification reaction.

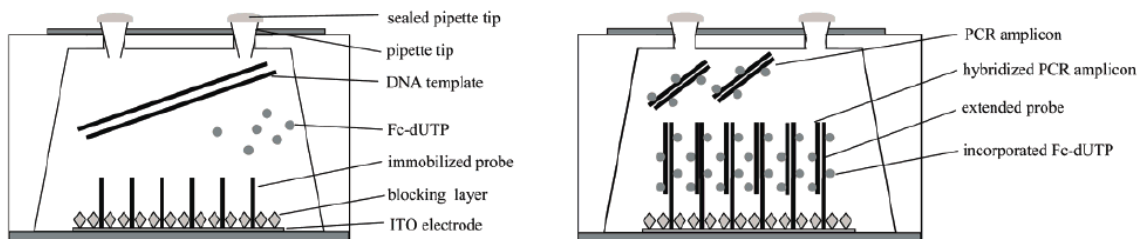


**Figure 1.11.** Microdevice for simultaneous PCR DNA amplification and real-time monitoring (Adapted from [50]).

#### 1.2.2.2. Immobilization-Free EC DNA Sensors with PCR

Tamiya and co-workers demonstrated the first immobilization-free EC scheme for PCR amplicon detection [43]. After PCR, the reaction mixture was mixed with a redox indicator (Hoechst 33258). In the absence of a target sequence, no PCR amplicons were produced. When the mixture was placed onto a glassy carbon electrode, the redox indicator diffused freely to the electrode surface and anodic current signal was measured. While in the presence of the target sequence, PCR amplicons were produced. The redox indicator, which is a minor groove binder, complexed to the amplicons and the anodic current signal was lower than that of the uncomplexed ones due to a significant

reduction in the diffusion coefficient. The same group applied this scheme for single-nucleotide polymorphism (SNP) detection (Figure 1.12) [51].

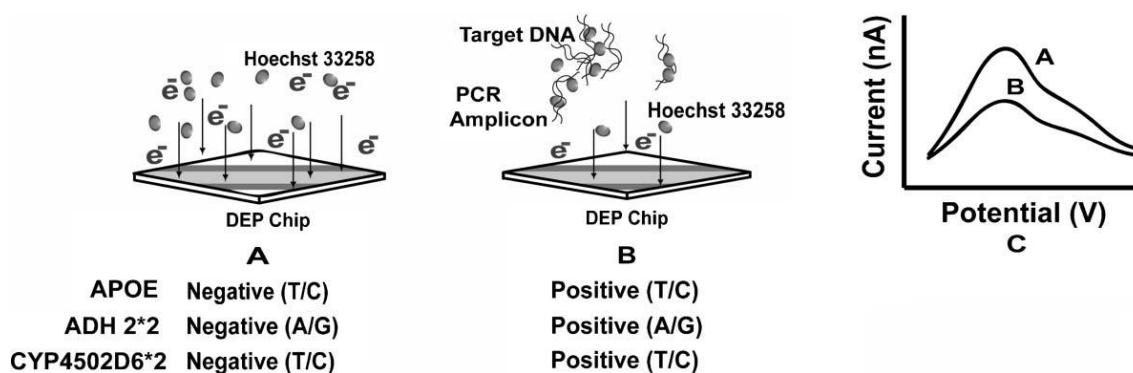


**Figure 1.12.** Immobilization-free EC detection of PCR amplicons using Hoechst 33258 (Adapted from [51]). (A) Freely moving Hoechst 33258 favors EC transduction; (B) Binding of Hoechst 33258 to DNA inhibits the EC transduction; (C) EC signal suppressed by target DNA.

As mentioned in Section 1.1.2, Hsing and co-workers utilized Fc-PNA for immobilization-free EC DNA detection [44]. In fact, in addition to oligonucleotide target, they also demonstrated the detection of unpurified PCR amplicons. With target amplification, the sensitivity was enhanced about  $10^5$ -fold.

The EC measurements of the two above-mentioned examples were conducted after PCR. Real-time PCR monitoring with immobilization-free EC scheme was first reported by Gong and co-workers [52]. A microchannel in polydimethylsiloxane (PDMS) was

fabricated, which was sealed by a glass substrate with an array of patterned Pt electrodes for EC measurements (Figure 1.13). A PCR mixture in the microchannel was transported repeatedly through three temperature zones. A redox indicator (MB) was included in the PCR mixture. Upon target amplification, MB intercalated with the amplicons, which significantly slowed down its diffusion to the electrode surface and thus the EC signal was suppressed. It should be noted that detection electrodes were placed at different thermal cycles, enabling real-time PCR monitoring.

Limoges and co-workers reported another real-time immobilization-free EC detection scheme based on catalytic oxidation of 2'-deoxyguanosine 5'-triphosphate (dGTP) by  $\text{Ru}(\text{bpy})_3^{3+}$  (bpy = 2,2'-bipyridine) or 7-deaza-dGTP by  $\text{Os}(\text{bpy})_3^{3+}$  [53]. A custom-made PCR and EC detection container was used so that temperature cycling was achieved by a conventional thermal cycler (Figure 1.14). During PCR amplification, the amount of free dGTP or 7-deaza-dGTP decreased as a result of its incorporation into PCR amplicons. The EC detection system (with screen-printed carbon working and counter electrodes and silver/silver chloride (Ag/AgCl) reference electrode) oxidized  $\text{Ru}(\text{bpy})_3^{2+}$  or  $\text{Os}(\text{bpy})_3^{2+}$  at the electrode surface, which in turn oxidized dGTP or 7-deaza-dGTP, respectively, and itself reduced back to  $\text{Ru}(\text{bpy})_3^{2+}$  or  $\text{Os}(\text{bpy})_3^{2+}$ . This catalytic recycling formed the basis of the EC measurements. It should be emphasized that the incorporated dGTP or 7-deaza-dGTP was less oxidizable due to steric hindrance and smaller diffusion coefficient. Therefore, the EC signal became smaller as more dGTP or 7-deaza-dGTP were consumed in the course of target amplification.

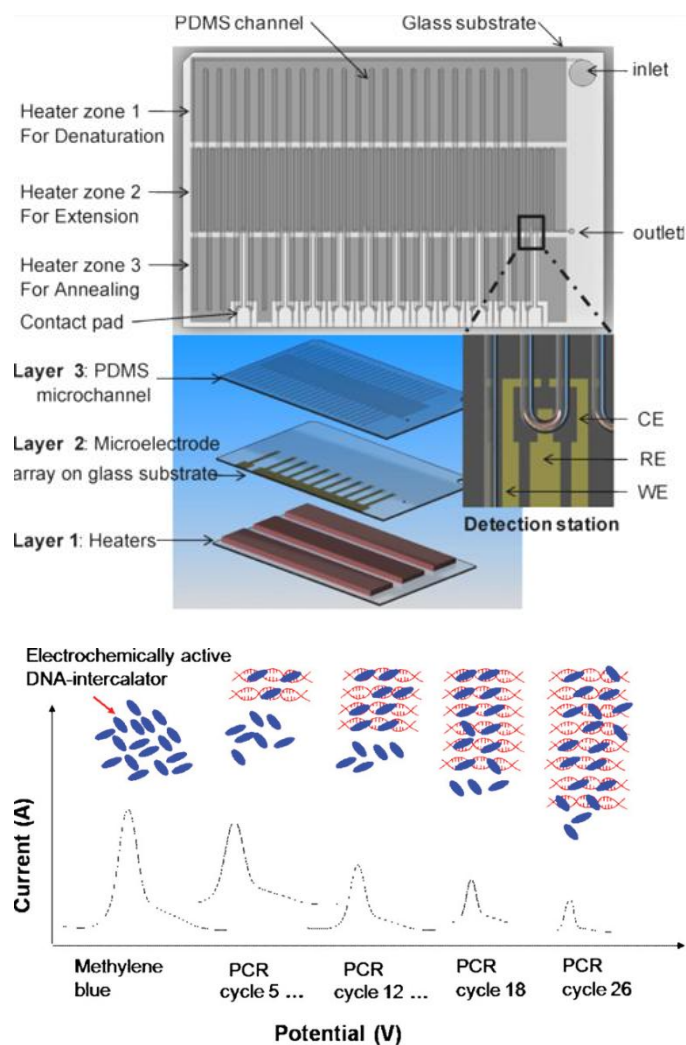


**Figure 1.13.** (Top) Layout of the integrated continuous-flow PCR and EC detection microchip and (bottom) EC detection scheme utilizing MB as redox indicator (Adapted from [52]).

The same group also demonstrated another real-time immobilization-free EC detection scheme based on a redox indicator ( $\text{Os}[(\text{bpy})_2\text{DPPZ}]^{2+}$ , DPPZ = dipyrido[3,2-a:2',3'-c]phenazine) (Figure 1.15) [54]. Prior to target amplification, the redox indicator

diffused freely to the electrode surface (the same custom-made PCR and EC detection container mentioned above). When PCR amplicons were generated, the redox indicator intercalated with the amplicons and thus the amount of free redox indicator decreased, resulting in a decrease in EC signal. Besides, it should be noted that the amplicon-bound redox indicator gave rise to a lower EC signal as discussed earlier.

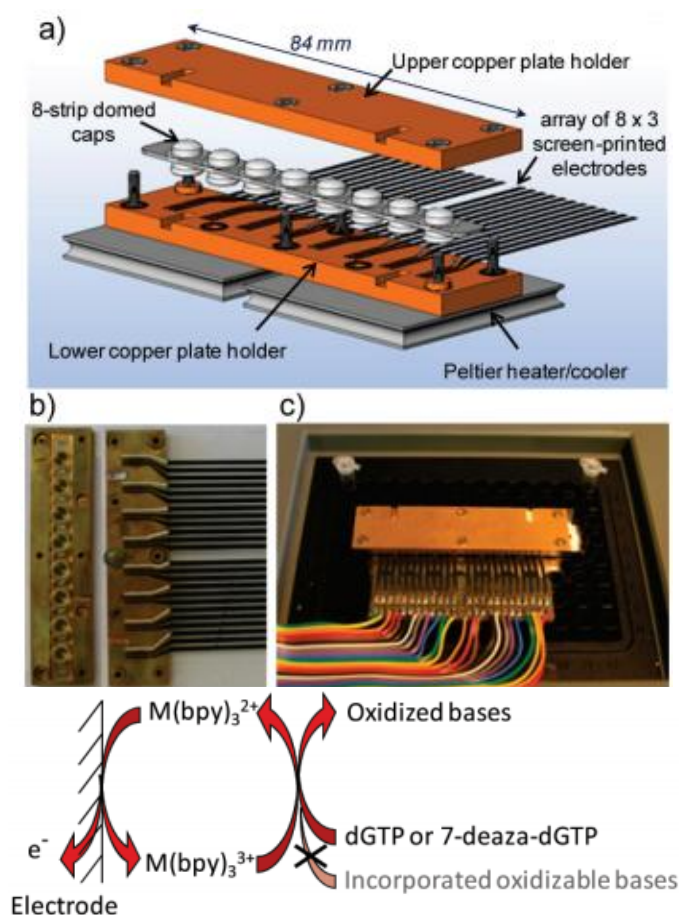


**Figure 1.14.** (Top, a–c) Layout of the custom-made EC cells for real-time PCR monitoring and (bottom) EC detection scheme based on catalytic oxidation of dGTP or 7-deaza-dGTP (Modified from [53]).

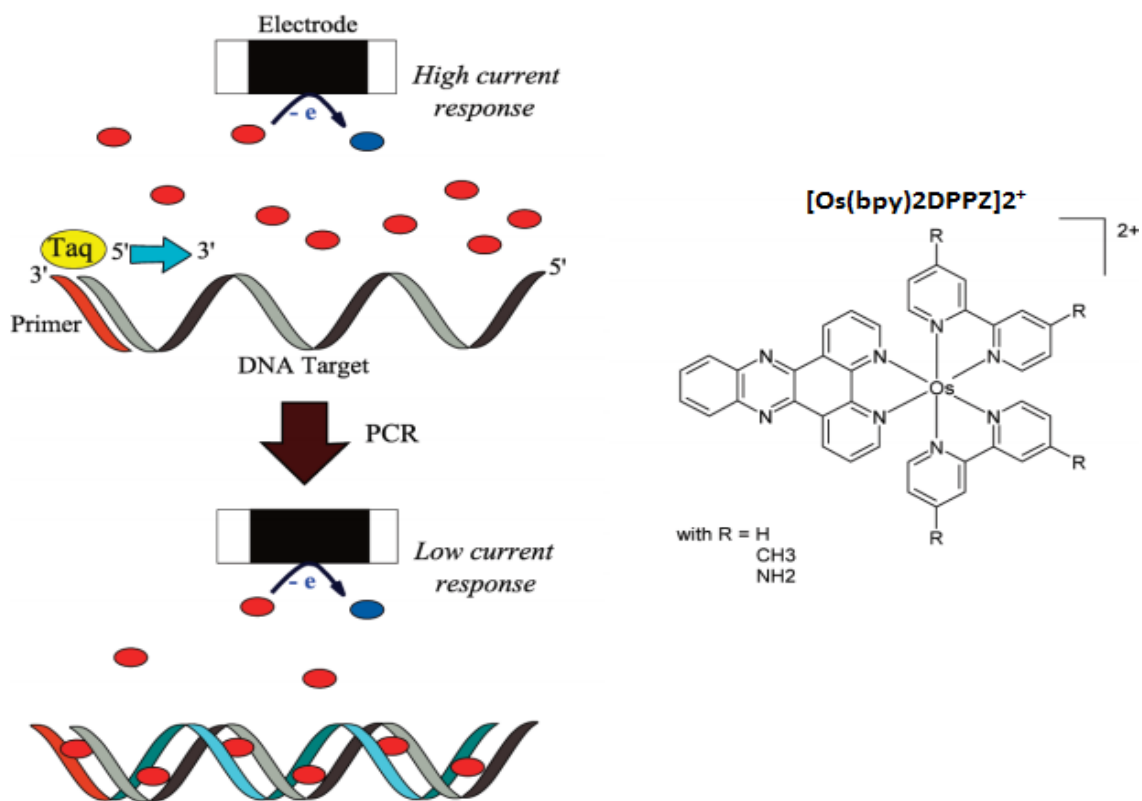


**Figure 1.15.** Schematic illustration of real-time immobilization-free EC detection scheme based on redox intercalator of  $[\text{Os}(\text{bpy})_2\text{DPPZ}]^{2+}$  (Adapted from [54]).

Hsing and co-workers demonstrated the use of a MB-labeled hydrolysis probe (termed as eTaq probe) for immobilization-free EC PCR detection (Figure 1.16) [55]. The eTaq probe was complementary to a specific PCR amplicon region and the redox label (MB) was attached to the 5'-end of the oligonucleotide. With ITO working electrode, the intact eTaq probe could not approach the electrode surface due to electrostatic repulsion (both are negatively charged). Upon the generation of PCR amplicons, the eTaq probe

hybridized with the denatured template/amplicon during the primer annealing step. Next, during the extension step, the eTaq probe was hydrolyzed by Taq DNA polymerase's 5'→3' exonuclease activity, producing small fragments of the probe. The MB-labeled fragment was detectable by the ITO electrode attributed to reduced electrostatic repulsion and faster diffusion. In their work, PCR was carried out in a conventional thermal cycler, and at different cycles, samples were pipetted out and placed onto the EC detection platform.

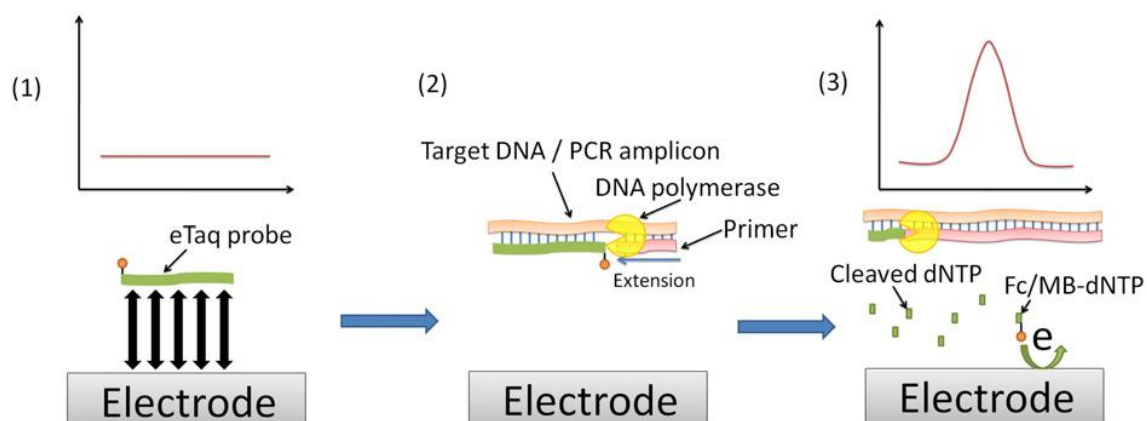


**Figure 1.16.** Immobilization-free EC detection scheme using eTaq probe (Adapted from [55]).

### 1.2.3. Isothermal Amplification

Various isothermal DNA amplification strategies have been devised in the last two decades including strand displacement amplification [56], rolling circle amplification (RCA) [57-58], loop-mediated isothermal amplification (LAMP) [59], helicase-

dependent amplification [60], strand-displacement polymerization reaction [61], primer generation–rolling circle amplification (PG–RCA) [62], etc. These isothermal strategies require simpler heating instrumentation than that of PCR, facilitating point-of-care and on-site DNA amplification. In these strategies, several DNA polymerases are used to amplify target sequences, the majority of which have strand displacement property. Alternatively, endonuclease [63-64] or exonuclease [65-67] can be employed for signal-amplified isothermal DNA detection.

RCA was independently invented by two research groups in mid 1990s that amplifies DNA in a linear fashion [57-58]. As shown in Figure 1.17, RCA consists of a circular ssDNA template, a short DNA primer which is complementary to a portion of the circular template, and a thermostable DNA polymerase to polymerize dNTPs into a ssDNA molecule having hundreds to thousands of repeats of complementary sequence of the circular template. RCA can be performed by a number of thermostable DNA polymerases which lack exonuclease activity but with strand displacement activity, such as phi29 DNA polymerase, Bst DNA polymerase, Klenow Fragment ( $3' \rightarrow 5'$   $\text{exo}^-$ ), and Vent ( $\text{exo}^-$ ) DNA polymerase [68]. When combined with padlock probe, RCA was successfully utilized for SNP detection [69-70]. In terms of amplification reaction/product quantification, colorimetric [71-73], fluorescence [63,74], and EC [75-76] techniques have been demonstrated. Examples of EC DNA sensors with RCA are described in the next section.

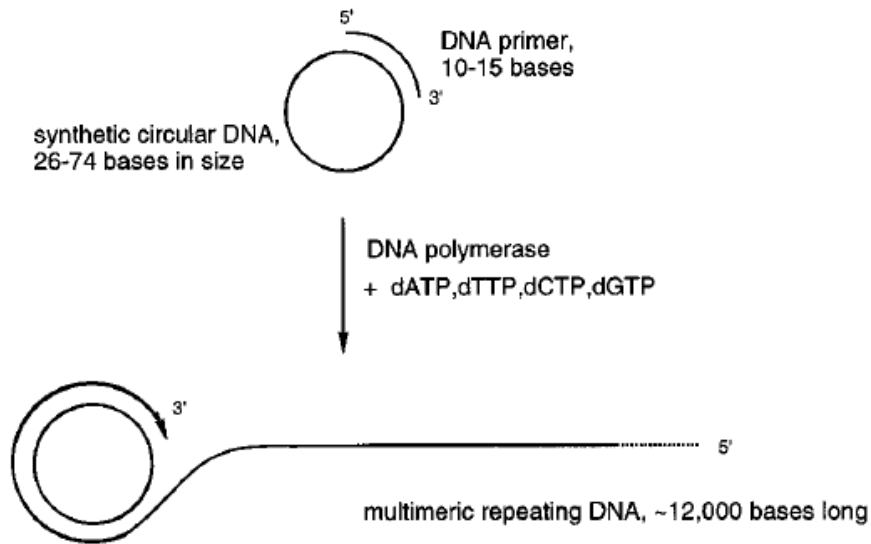


**Figure 1.17.** Schematic illustration of RCA (Modified from [58]).

LAMP was introduced by Notomi and co-workers that amplifies DNA exponentially [59]. As shown in Figure 1.18, four primers that recognize six regions of a target are used. A first inner primer initiates the reaction, and then the extended first inner primer is displaced by a first outer primer. In fact, the first inner primer has an overhang sequence that hybridizes with an adjacent region downstream of the first inner primer to form a stem-loop structure. A second inner primer and outer primer hybridize to the extended first inner primer, and the extended and displaced second inner primer adopts a two-end stem-loop structure. Subsequently, the inner primers hybridize to the loop for cycling amplification to continue. The reaction products are dsDNA with alternately inverted repeats of the target sequence in the same strand. Typically,  $10^9$  copies of the target sequence are produced in one hour. The same research group also achieved a

faster reaction by utilizing two additional primers [77]. Despite its high sensitivity and specificity, LAMP requires sophisticated primer design.

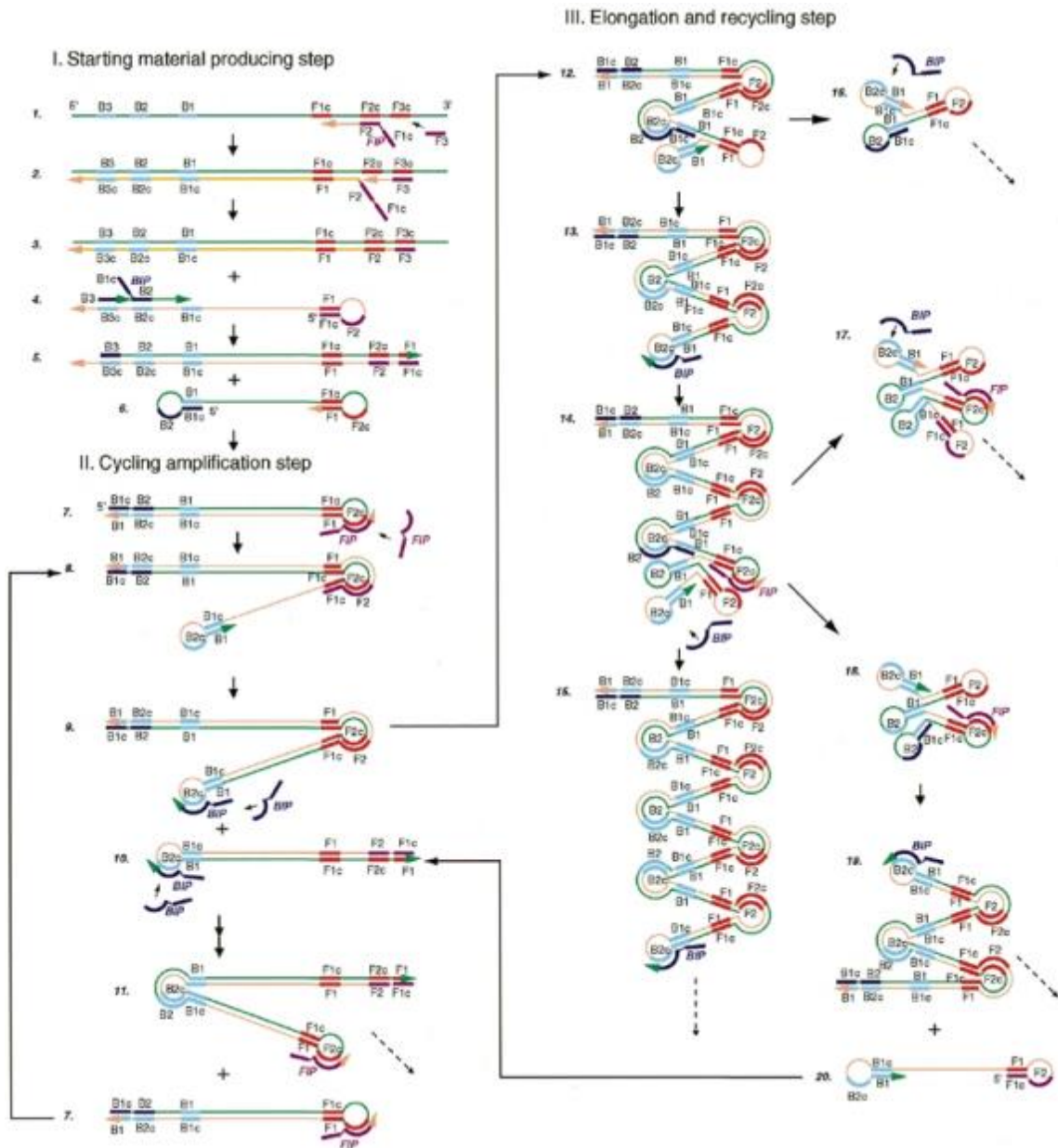


**Figure 1.18.** Schematic illustration of LAMP (Adapted from [59]).

Strand-displacement polymerization reaction was introduced by Wang and co-workers in 2009 that amplifies DNA in a linear fashion [61]. The reaction makes use of a hairpin probe (i.e., molecular beacon, stem-loop structure, functionalized with a fluorophore and a quencher at its two ends), a primer, and DNA polymerase (Klenow Fragment ( $3' \rightarrow 5'$  exo<sup>-</sup>)). As shown in Figure 1.19, the loop sequence hybridizes with a complementary target DNA sequence, which in turn separates the stem as well as the fluorophore and quencher. An increase in fluorescence signal is thus observed. Then, the primer hybridizes to the stem region (3'-end of the beacon), followed by extension and strand displacement reactions. As a result, the displaced target is recycled for further rounds of amplification.

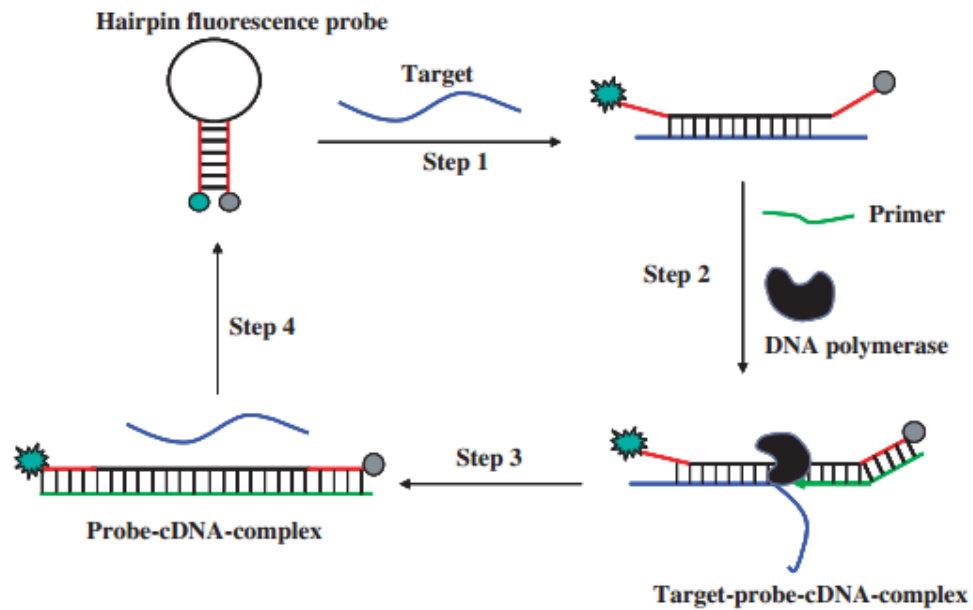


**Figure 1.19.** Schematic illustration of isothermal circular strand displacement polymerization reaction (Adapted from [61]).

PG-RCA was reported by Komiyama and co-workers in 2009 that greatly improves the sensitivity of RCA by adding a nicking enzyme (Figure 1.20) [62]. In PG-RCA, nicking sites are incorporated into RCA-generated long chain ssDNA, which hybridizes with the circular templates and is then nicked to generate new primed circular templates. Hence, target amplification proceeds in an exponential manner. It was reported that the detection limit was down to 84.5 yoctomole (or 50.7 molecules). A similar strategy was reported by Hollfelder and co-workers in 2010 [78]. A circular dsDNA is amplified to generate linear dsDNA products by T4 replisome, nicking endonuclease, and a reverse primer.

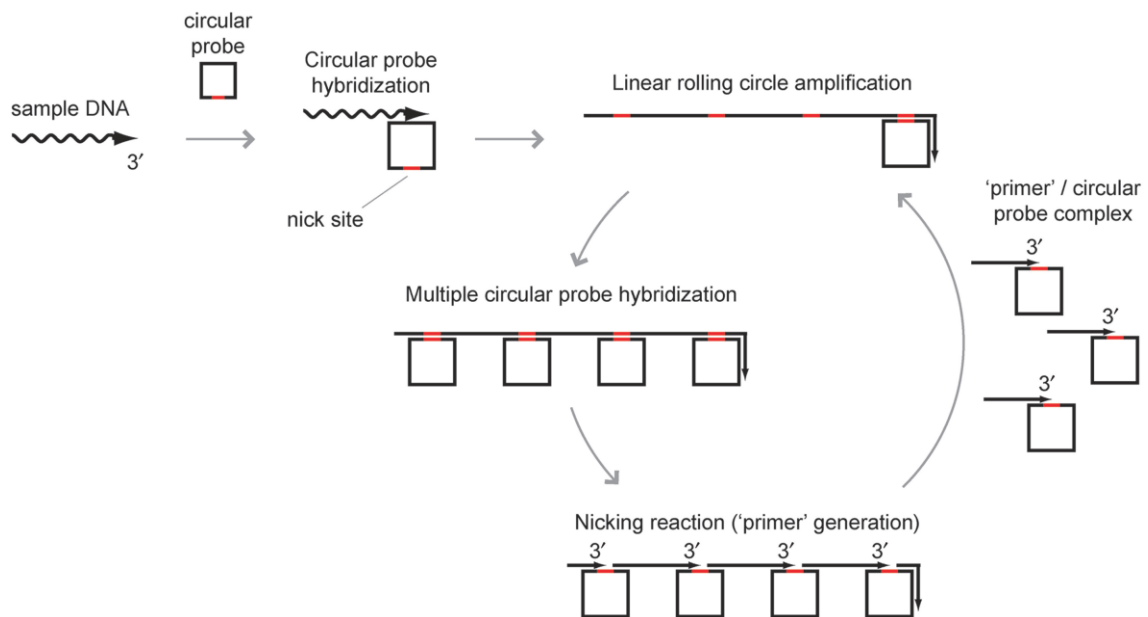


**Figure 1.20.** Schematic illustration of PG-RCA (Adapted from [62]).

### 1.2.4. EC DNA Sensors with Isothermal Amplification

There has been increasing interest in integrating EC DNA sensors with isothermal amplification over the past few years. They can be grouped into immobilization-based and immobilization-free approaches, as discussed in detail below.

#### 1.2.4.1. Immobilization-Based EC DNA Sensors with Isothermal Amplification

Willner and co-workers demonstrated an immobilization-based EC platform for circular viral DNA detection using RCA reaction (Figure 1.21) [76]. A gold electrode immobilized with a capture probe was used. A target circular viral DNA hybridized to

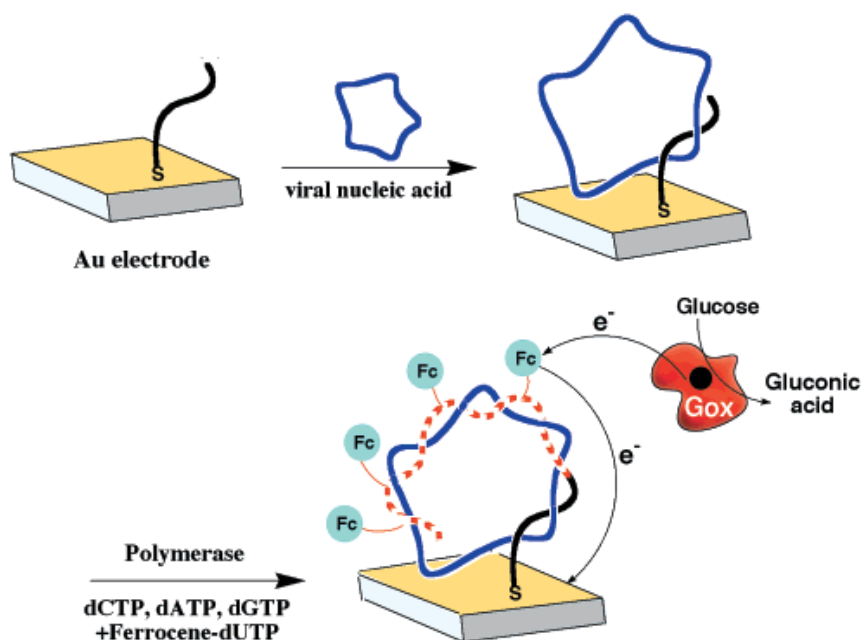


**Figure 1.21.** Immobilization-based EC detection of viral DNA with RCA using Fc-dUTP redox marker and enzymatic signal amplification (Adapted from [76]).

the capture probe and triggered RCA reaction. The RCA reaction product was labeled with Fc redox marker via Fc-dUTP incorporation. Moreover, glucose oxidase-based catalytic recycling of the oxidized Fc was employed to amplify the EC signal.

Shen and co-workers demonstrated another immobilization-based EC DNA platform with RCA (Figure 1.22) [75]. A padlock probe was used to recognize SNP targets.

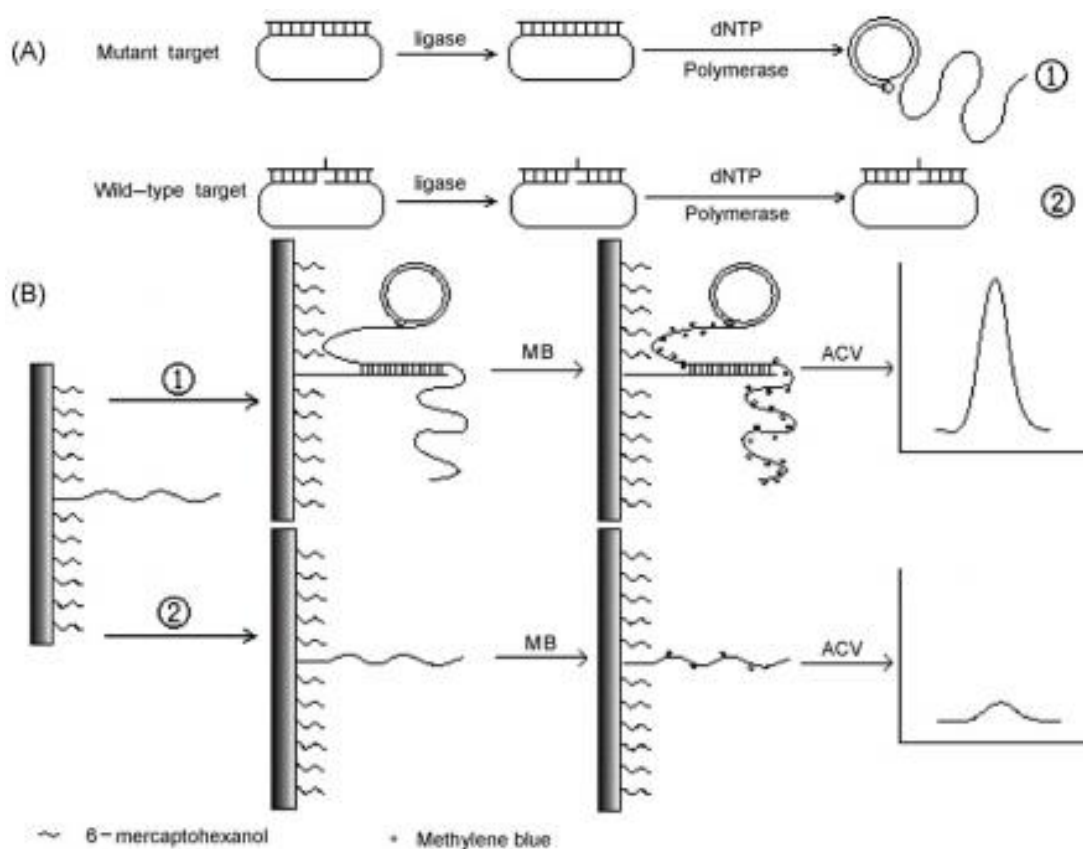


**Figure 1.22.** Immobilization-based EC DNA detection with ligation and RCA using MB redox indicator (Adapted from [75]). (A) Schematic illustration for SNP detection; (B) Hybridization of RCA amplicons to immobilized probe for EC signal detection.

When the target was perfectly complementary to the padlock probe, ligation reaction produced a circular template. This was followed by RCA reaction to generate a long ssDNA product. A probe-immobilized gold electrode was used to capture the RCA reaction product. Then, a redox marker (MB) was added. With more MB bound to the capture probe–RCA product hybrid than to the capture probe, a larger EC signal was observed.

#### **1.2.4.2. Immobilization-Free EC DNA Sensors with Isothermal Amplification**

In 2009, Tamiya and co-workers reported the first immobilization-free EC DNA sensor with isothermal amplification [79]. In their work, a custom-made reaction and detection tube was used, as shown in Figure 1.23. The reaction zone was separated from the EC detection zone by a mechanical valve. The former one contained a LAMP reaction mixture and the latter one contained a redox indicator solution (Hoechst 33258) as well as EC detection electrodes (screen-printed carbon working and counter electrodes and Ag/AgCl reference electrode). LAMP reaction was carried out by placing the reaction zone into a constant-temperature heat-block. After the amplification reaction, the tube was taken out of the heat-block and the valve was open to allow mixing of the LAMP reaction mixture and Hoechst 33258. In fact, the same group utilized Hoechst 33258 for immobilization-free EC detection of PCR amplicon, as discussed in Section 1.2.2.2. As a result of the binding of Hoechst 33258 to the minor groove of the LAMP reaction products, a decrease in the anodic current peak was observed. It should be noted that

only end-point measurement was made due to the post-amplification mixing with the redox indicator.

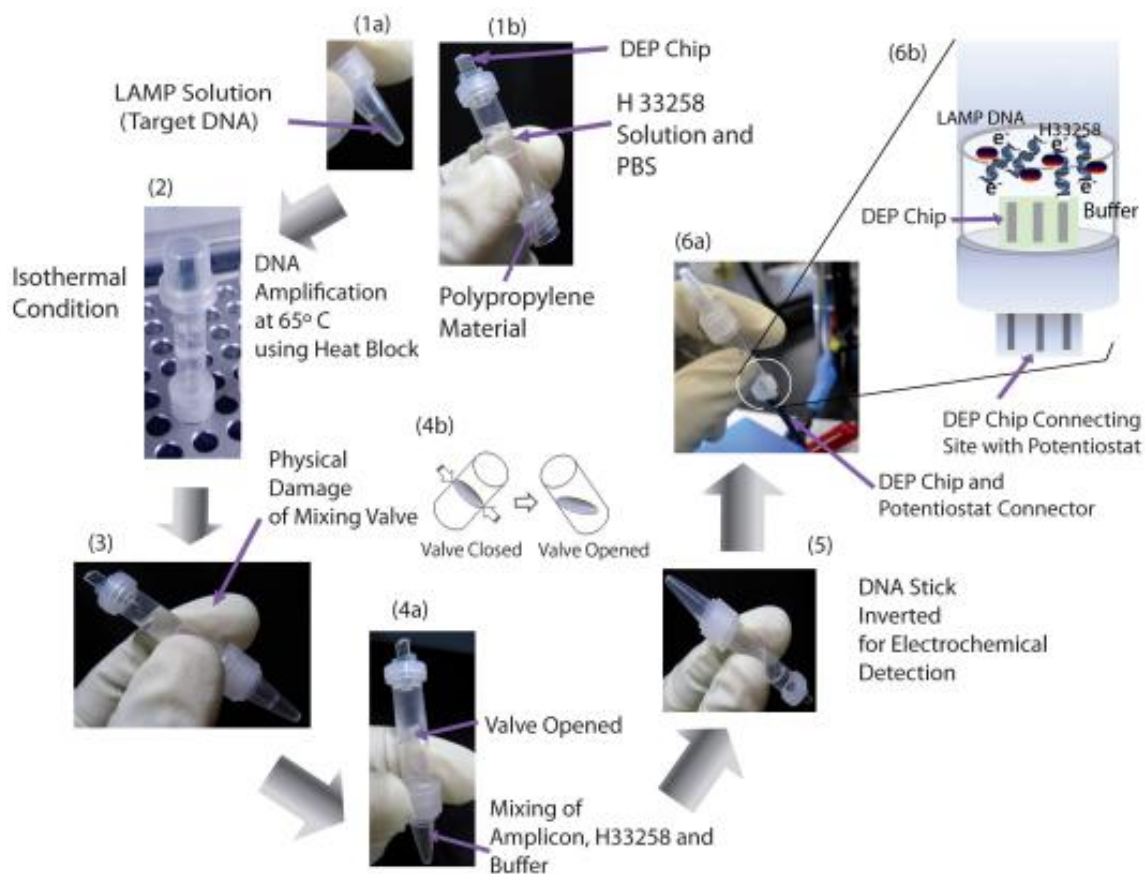


**Figure 1.23.** Immobilization-free EC DNA sensor with LAMP utilizing Hoechst 33258 (Adapted from [79]).

Zhang and co-workers performed EC analysis of LAMP reaction products by direct oxidation of free dGTP using carbon nanotube array electrode [80]. In the presence of a target sequence, LAMP reaction proceeded and dGTP was incorporated into dsDNA products. This resulted in a decrease in the anodic current peak as dsDNA diffuses

slower to the electrode surface than free dGTP. Besides, the incorporated dGTP is less oxidizable than free dGTP due to base pairing. The authors demonstrated the EC monitoring of the LAMP reaction at 5-min intervals by dipping the 3-electrode detection system into the reaction mixture. It should be noted that the working electrode was taken out from the reaction mixture after every scan for surface regeneration.

Hsing and co-workers reported an immobilization-free EC DNA sensor with strand-displacement polymerization reaction [81]. As shown in Figure 1.24, an Fc-PNA probe, a molecular beacon, a primer, DNA polymerase with strand displacement property, and an ITO electrode were used. In the absence of a target sequence, the Fc-PNA probe hybridized with the 5'-overhang of the beacon and thus could not approach the electrode surface. On the other hand, the hybridization of the target with the beacon-Fc-PNA hybrid allowed the primer to hybridize to 3'-end of the beacon, which triggered the primer extension reaction and displacement of the Fc-PNA probe as well as the target. The displaced Fc-PNA probe gave rise to an anodic current peak. The displaced target was capable of initiating next round of hybridization, extension, and displacement.

Plaxco and co-workers developed an immobilization-free EC DNA sensor with LAMP based on MB redox indicator (Figure 1.25) [82]. When MB intercalated with the LAMP reaction products, the redox current decreased due to slower diffusion of the complex than free MB. Real-time detection was achieved in their work by passivating a gold working electrode with mercaptohexanol.

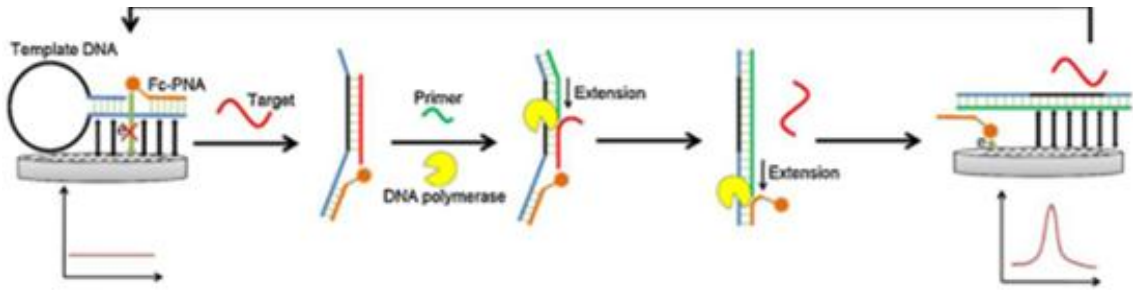


**Figure 1.24.** Immobilization-free EC DNA sensor with strand-displacement polymerization reaction using Fc-PNA probe (Adapted from [81]).

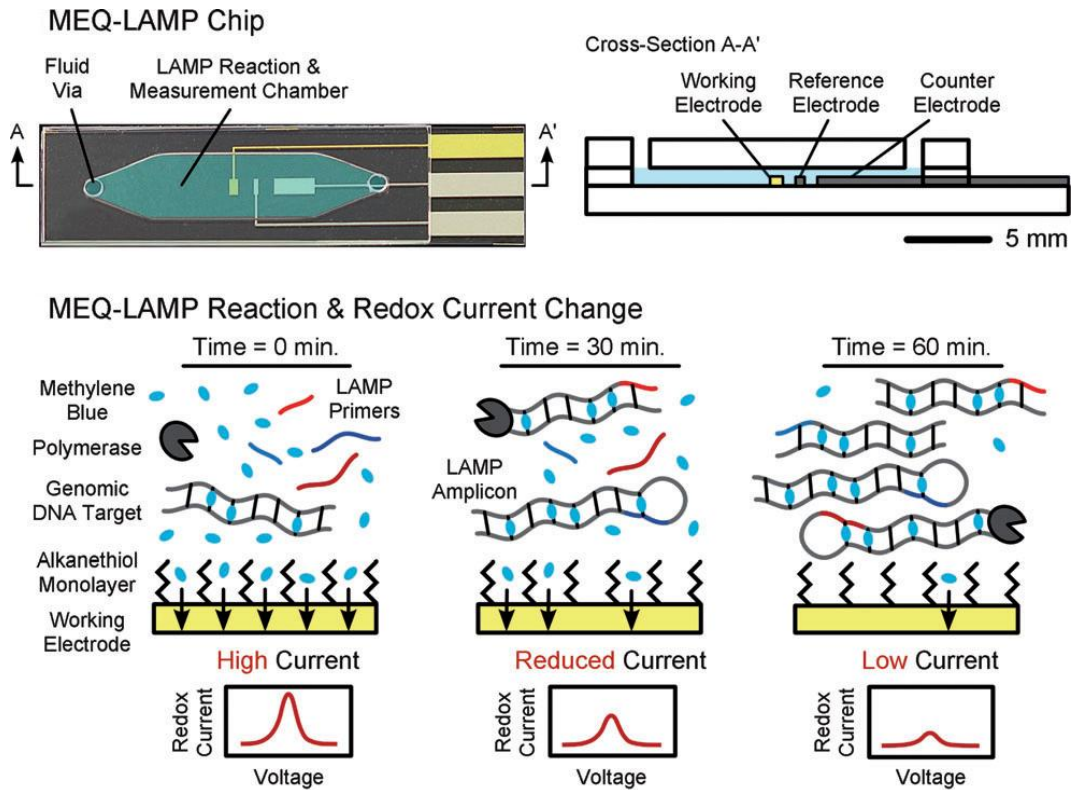


**Figure 1.25.** Immobilization-free EC DNA sensor with LAMP using MB redox indicator (Adapted from [82]).

### **1.3. Current Limitations**

EC DNA sensors hold great promise for point-of-care and on-site applications. Nevertheless, until now, their practical usage has been very limited. There are several key limitations of the current approaches. The immobilization-based EC DNA sensors require the use of costly modified oligonucleotides as well as time-consuming and laborious electrode functionalization. The immobilization-free EC DNA sensors, though simple in electrode preparation, suffers from low sensitivity. In view of this, efforts have been made to integrate with PCR (particularly in microchip format for achieving portable devices), but the device fabrication and thermal cycling control adds further complications. To further simplify the assay system, immobilization-free EC DNA sensors have been coupled with isothermal amplification. Until now, the coupled systems have only employed LAMP for exponential isothermal amplification. One main disadvantage of LAMP is the complicated primer design (at least four primers). With these limitations, new EC DNA detection systems that are simple (assay design, preparation, and instrumentation) and sensitive have yet to be realized.

### **1.4. Objectives of the Study**

The main goal of this study is to develop a simple and sensitive EC DNA detection system. In this study, PG-RCA is employed to achieve isothermal exponential amplification and immobilization-free EC DNA detection is achieved using MB as redox indicator along with an ITO working electrode. One objective of this work is to

evaluate the performance of the immobilization-free EC DNA sensors with PG-RCA (exponential amplification) as compared with RCA (linear amplification). Another objective is to determine the specificity and sensitivity of this new detection scheme. The sensitivity of the immobilization-free EC detection scheme is compared with that of the fluorescence technique (using fluorescent stain for nucleic acid, SYBR<sup>®</sup> Gold). Yet another objective is to investigate electrode fouling by the PG-RCA reaction mixture. Simple electrode regeneration is explored to enable EC measurements at different time points of the PG-RCA reaction using the same electrode. Lastly, the use of molecular beacon probe for generic sequence recognition, rather than sequences at 3'-end, is studied.

## Chapter 2

### Methodology

The detection scheme of the immobilization-free EC DNA sensor with PG-RCA is introduced in Section 2.1. The reagents and instrumentation used in the experiments are listed in Section 2.2. The experimental protocols are given in Section 2.3.

#### 2.1. Detection Scheme

The immobilization-free EC DNA detection scheme, its combination with PG-RCA, and the use of molecular beacon as target recognition probe as well as primer for PG-RCA are described in this section.

##### 2.1.1. Immobilization-Free EC DNA Detection Scheme

MB, a DNA intercalator, is employed as the redox indicator [13,52,75,82]. In fact, MB binds preferentially to ssDNA (through interaction with G base) than to dsDNA (hybridized G base, i.e., base-paired with C base, are less accessible) [52,75,83-84]. As shown in Figure 2.1, in the absence of ssDNA, the MB molecules diffuse freely to an electrode surface, enabling electron transfer and thus a redox signal is obtained. On the other hand, the MB molecules bind to ssDNA and their diffusion to the electrode surface is retarded (as a result of a smaller diffusion coefficient than the free MB molecules), leading to a reduction of the electron transfer and the redox signal decreases. To achieve

a greater change in the MB redox signal upon binding to ssDNA, an ITO working electrode is utilized. The electrostatic repulsion between the ITO electrode and the MB–ssDNA complex (both are negatively charged) further hinders the redox indicator from approaching the electrode surface.

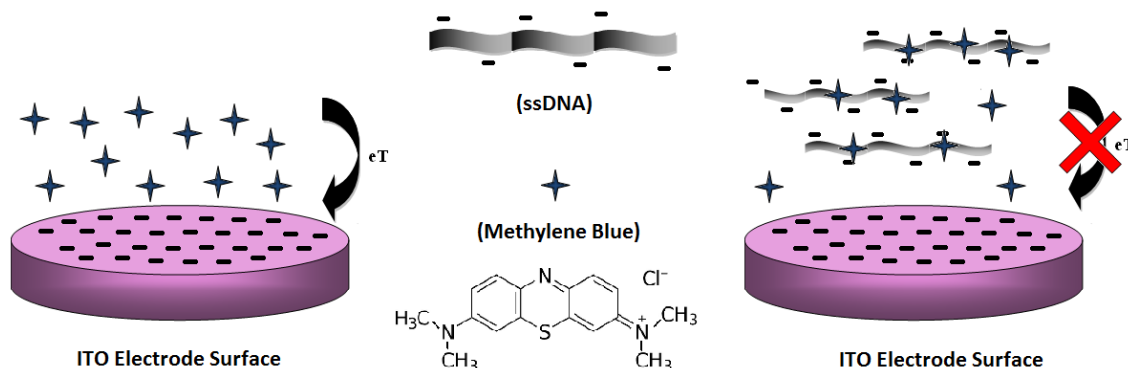


**Figure 2.1.** Immobilization-free EC DNA detection scheme using MB.

DPV is used for the EC measurements. DPV's voltage waveform is constructed by the superposition of a staircase wave and a pulse wave (Figure 2.2). Two current samplings are performed in each cycle (i.e., right before and close to the end of the pulse). The difference of the two current readings minimizes the capacitive current effect. A peak-shaped voltammogram is obtained by plotting the current difference as a function of the scanning potential. DPV offers highly sensitive EC measurement of redox indicators and has thus been extensively utilized in EC DNA sensors.

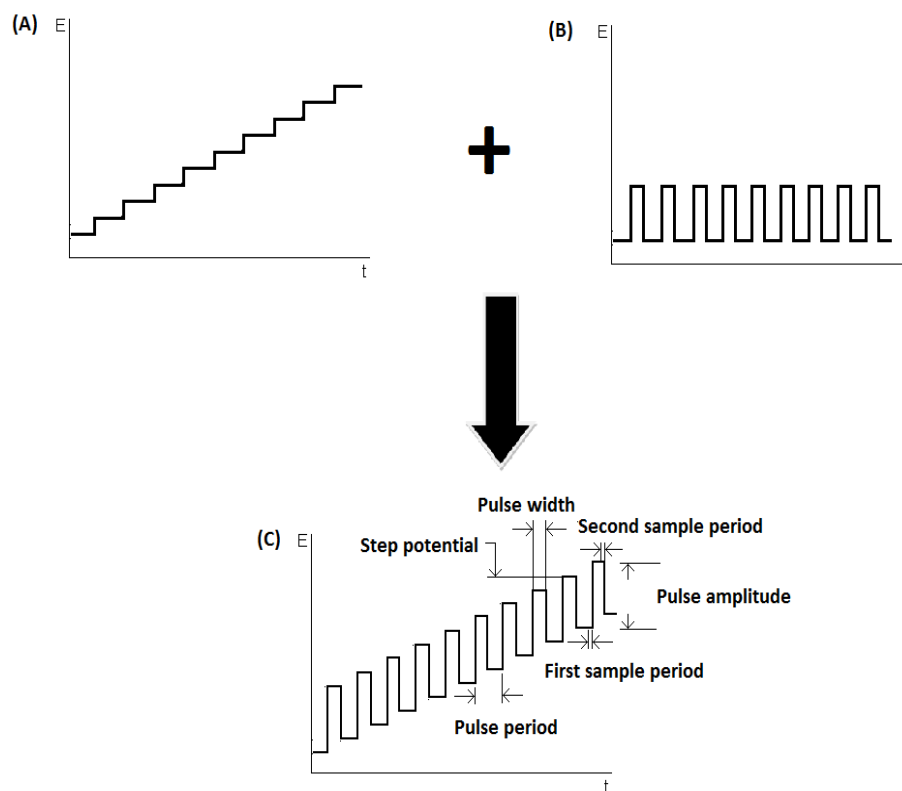


**Figure 2.2.** Schematic illustration of DPV waveform. (A) Linear staircase wave; (B) Regular pulse wave; (C) Differential pulse wave.

### **2.1.2. Immobilization-Free EC DNA Detection Scheme Combined with PG-RCA**

PG-RCA is utilized as the isothermal DNA amplification method in this study. Figure 2.3 shows the immobilization-free EC DNA detection scheme combined with PG-RCA using MB redox indicator. When a target sequence hybridizes to a circular ssDNA template at its 3'-end, RCA is triggered and long ssDNA amplicon is generated. When the ssDNA amplicon hybridizes with the circular template, the former one is nicked,

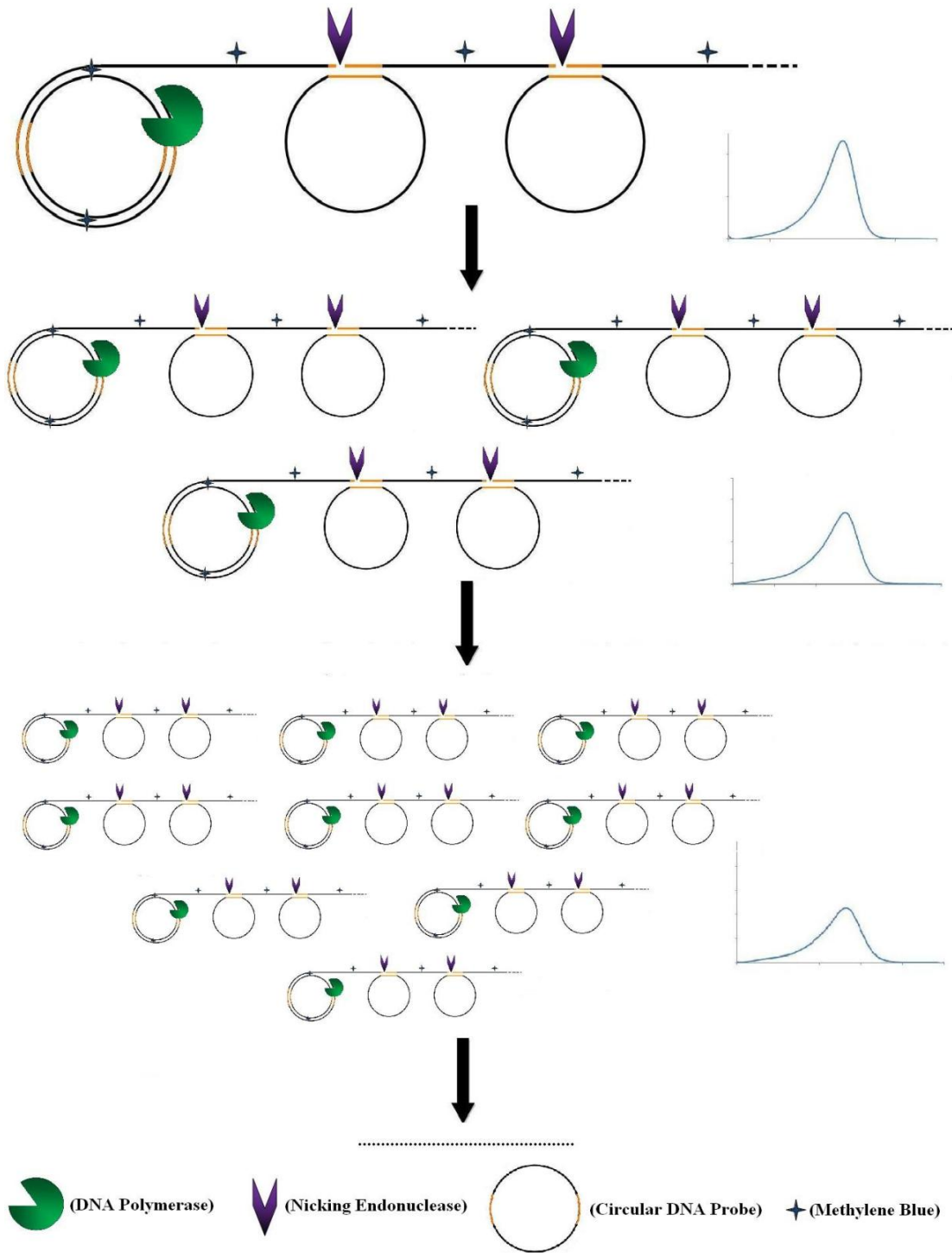


**Figure 2.3.** The immobilization-free EC detection scheme combined with PG-RCA.

which serves as new primed site for extension. Repeated rounds of circular template hybridization, nicking, and extension produce ssDNA products in an exponential manner. It should be noted that MB is included in the PG-RCA reaction mixture. As discussed in the previous section, the MB molecules bind to the ssDNA products and a low redox current is obtained using an ITO working electrode.

### 2.1.3. PG-RCA with Molecular Beacon

A molecular beacon is designed for the detection of target sequence located not at the 3'-end. As shown in Figure 2.4, in the absence of a target sequence, the beacon is at its stem-loop structure and no PG-RCA occurs. While in the presence of the target, the stem is dehybridized, which in turn allows its 3'-portion to hybridize to the circular template and thus PG-RCA reaction is triggered.

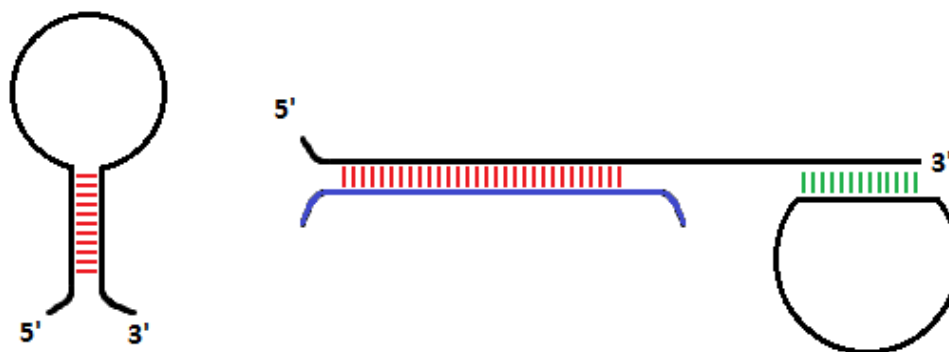


**Figure 2.4.** Schematic illustration of molecular beacon as target recognition probe as well as primer for PG-RCA reaction. The target sequence is marked in blue.

## 2.2. Materials and Instrumentation

The reagents, oligonucleotide sequences, instrumentation, and electrodes are listed in this section.

### 2.2.1. Reagents

Alconox, propan-2-ol, sulphuric acid ( $\text{H}_2\text{SO}_4$ ), hydrogen peroxide ( $\text{H}_2\text{O}_2$ ), MB, tris(hydroxymethyl)aminomethane (Tris base), boric acid, and ethylenediaminetetraacetic acid (EDTA) were purchased from Sigma-Aldrich (St. Louis, MO, USA). Silicone elastomer and its curing agent were purchased from Dow Corning (Midland, MI, USA). CircLigase<sup>TM</sup> II ssDNA Ligase and Exonuclease I were purchased from Epicentre (Madison, WI, USA). QIAquick Nucleotide Removal Kit was purchased from QIAGEN (Valencia, CA, USA). RCA or PG-RCA reaction buffer (RB, 50 mM NaCl, 10 mM Tris-HCl, 10 mM  $\text{MgCl}_2$ , and 1 mM DTT, pH 7.4), phi29 DNA polymerase, Nb.BbvCI nicking endonuclease, dNTPs, low molecular weight DNA ladder, and bovine serum albumin (BSA) were purchased from New England Biolabs (Ipswich, MA, USA). SYBR<sup>®</sup> Gold and agarose were purchased from Invitrogen (Carlsbad, CA, USA). All enzymatic reaction solutions were prepared using UltraPure<sup>TM</sup> DNase/RNase-free distilled water from Invitrogen. All other solutions were prepared with ultrapure water (18.2 M $\Omega$  cm) from a Milli-Q Advantage A10 System (Millipore, Billerica, MA, USA).

## 2.2.2. Oligonucleotide Sequences

DNA oligonucleotides used in this study were purchased from Integrated DNA Technologies (Coralville, IA, USA) and were HPLC- or PAGE-purified. Their sequences are given in Table 2.1. The circular template sequence was phosphorylated at its 5'-end to allow self-ligation (i.e., circularization). Its analyte binding region is bolded and the recognition site for the nicking endonuclease to cleave ssDNA amplicon is underlined. The beacon's stem sequence is italicized and its 3'-end sequence is identical to the analyte sequence. The beacon target is complementary to the 5'-end of the beacon.

**Table 2.1.** Oligonucleotide sequences used in this study.

Oligonucleotide name	Sequence
Circular template (74 bp)	5'-Phos/ <b>GTG GTT GTC TTC TCC TCA GCT</b> CTA TCG GAT TTG TAT CTC <u>TCC TCA GCT</u> CTA TCG GAT TTG TAT CTC TAA <b>GCA GT</b> -3'
Analyte (14 bp)	5'-CAA CCA CAC TGC TT-3'
Non-complementary sequence (19 bp)	5'-TGG CGA ACT ACT TAC TCT A-3'
Beacon (60 bp)	5'- <i>GGT TGG TGT GGT TGG TTT CGT GTC GTT</i> CGG TTT TTT TTT TTT TTT <i>CCA ACC ACA CTG</i> CTT-3'
Beacon target (37 bp)	5'-AAA AAA ACC GAA CGA CAC GAA ACC AAC CAC ACC AAC C-3'

### **2.2.3. Instrumentation**

Absorbance measurements were performed using an Ultrospec™ 2100 pro UV/visible spectrophotometer (GE Healthcare, Piscataway, NJ, USA). Real-time fluorescence measurements were performed using an Applied Biosystems 7500 Real-Time PCR System (Applied Biosystems, Carlsbad, CA, USA). Thermal reactions were performed using a GeneAmp® PCR System 9700 (Applied Biosystems). Plasma treatment was performed using a Plasma Cleaner PDC 32G (Harrick Plasma, Ithaca, NY, USA). EC measurements were performed using an Autolab PGSTAT302N potentiostat/galvanostat (Metrohm Autolab, The Netherlands) controlled by General Purpose Electrochemical System (GPES) software (Metrohm Autolab, The Netherlands). Agarose gel electrophoresis result was visualized and recorded by a GeneGenius<sup>2</sup> gel imaging system controlled by GeneSnap software from Syngene (Frederick, MD, USA).

### **2.2.4. Electrode Chips**

Gold and ITO electrode chips (both with Pt as counter and pseudo-reference electrodes) were fabricated according to previous reported procedures [36,44]. Briefly, for gold electrode chips, glass substrate was first photolithographically patterned to define the working electrode (1-mm in diameter). This was followed by gold sputtering and a lift-off process. Then, using the same steps were used to pattern the Pt counter and pseudo-reference electrodes. For ITO electrode chips, ITO-coated glass was used and was

patterned by photolithography and etching. Subsequently, Pt counter and pseudo-reference electrodes were patterned as that for the gold electrode chips.

The ITO electrode chip was cleaned by sonication in 8 g/L Alconox solution for 15 min, followed by propan-2-ol for 15 min, and twice in water for 15 min. The gold electrode chip was cleaned in piranha solution (mixture of  $\text{H}_2\text{SO}_4$ : $\text{H}_2\text{O}_2$  in a volume ratio of 3:1). CAUTION: piranha solution is a strong oxidizing agent, and must be handled with great care in a fume hood).

An EC measurement container was made from PDMS. The silicone elastomer and curing agent were mixed in a mass ratio of 10:1 and poured onto a silicon substrate (a thickness of about 4 mm). Then, it was degassed under vacuum for 30 min, cured at 80 °C for 1 h, and peeled from the silicon substrate. It is cut into smaller pieces (about 4 mm × 4 mm). Then, a 4-mm diameter hole was punched through the PDMS, serving as the EC measurement container when bonded to the electrode chips. The bonding was assisted by a plasma treatment. The PDMS substrate was cleaned with once in propan-2-ol and twice in water for 15 min each under sonication, followed by drying in an oven at 80 °C for 1 h. It was then put inside the plasma cleaner. Vacuum pump was used to reduce the pressure of the chamber to enable plasma generation. The plasma cleaner was turned on to the highest power for 1 min. Immediately after taken out from the plasma cleaner, the electrode chip and the PDMS substrate were aligned, brought into contact, and bonded. The PDMS-bonded electrode chip is schematically illustrated in Figure 2.5.

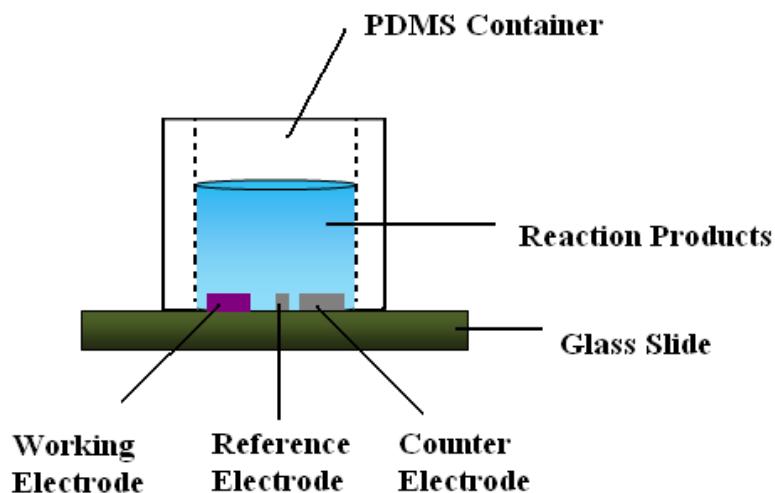


**Figure 2.5.** Schematic illustration of the PDMS-bonded electrode chip.

## 2.3. Experimental Protocols

### 2.3.1. Circular Template Preparation

The self-ligation of the circular template sequence was carried out according to the manufacturer's instructions. A 50- $\mu\text{L}$  reaction mixture with 1  $\mu\text{M}$  of the circular template sequence was incubated at 60  $^{\circ}\text{C}$  for 3 h. After the self-ligation reaction, it is heated to 80  $^{\circ}\text{C}$  for 10 min to inactivate the CircLigase<sup>TM</sup> II enzyme. Any unligated linear ssDNA sequence was digested by adding 20 units of Exonuclease I and incubating at 37  $^{\circ}\text{C}$  for 2 h, followed by 80  $^{\circ}\text{C}$  for 15 min to inactivate the Exonuclease I enzyme. The ligated circular template was purified by using the QIAquick Nucleotide Removal Kit. The concentration of the purified circular template was determined by the Beer–Lambert law:

$$A = \epsilon bC$$

where A is the absorbance (obtained using the UV/visible spectrophotometer),  $\epsilon$  is the extinction coefficient ( $672,200 \text{ M}^{-1}\text{cm}^{-1}$ ) for the circular template), b is the optical pathlength, and C is the concentration.

### **2.3.2. EC Measurement of MB with ssDNA**

A 10- $\mu\text{L}$  solution containing 20  $\mu\text{M}$  MB in RB, without or with 10  $\mu\text{M}$  ssDNA (beacon target), was introduced to the electrode chip. DPV measurements were performed with 50 ms modulation time, 200 ms interval time, 5 mV step potential and 100 mV modulation amplitude. The potential was scanned from  $-0.7 \text{ V}$  to  $-0.3 \text{ V}$  and the total EC measurement time was 16 s. Another set of experiments were performed with different concentrations of MB (1, 5, 10, 20, 50, and 100  $\mu\text{M}$ ) in the presence of 10  $\mu\text{M}$  ssDNA (beacon target).

### **2.3.3. Real-Time Fluorescence Measurement of PG–RCA**

The efficiency of the PG–RCA assay was evaluated quantitatively by real-time fluorescence measurement. A 20- $\mu\text{L}$  solution mixture containing RB, 0.2 mg/mL BSA, 50 nM circular template, 0.4 units phi29 DNA polymerase, 4 units Nb.BbvCI, 50  $\mu\text{M}$  dNTPs,  $0.1 \times$  SYBR<sup>®</sup> Gold, and analyte (0, 1 pM, 10 pM, 100 pM, and 1 nM) was incubated at 37  $^{\circ}\text{C}$  for 3 h. The measurement was performed every 2 min. RCA was also performed with 1 nM analyte, except without Nb.BbvCI, all other reaction components were the same as PG–RCA.

#### **2.3.4. Effect of MB on PG–RCA**

The effect of MB on PG–RCA was evaluated qualitatively by agarose gel electrophoresis. A 10- $\mu$ L solution mixture containing RB, 0.2 mg/mL BSA, 50 nM circular template, 0.2 units phi29 DNA polymerase, 2 units Nb.BbvCI, 50  $\mu$ M dNTPs, 20  $\mu$ M MB, and analyte (0 or 1 nM) was incubated at 37 °C for 2.5 h, followed by 80 °C for 15 min to inactivate the enzymes. Similarly, by excluding Nb.BbvCI, the effect of MB on RCA was also studied. It should be noted that a 10-fold higher concentration of the analyte (10 nM) than that in PG–RCA was used. The reaction products were analyzed by a 3% agarose gel (prepared in 0.5 $\times$  TBE buffer: 44.5 mM Tris base, 44.5 mM boric acid, 20 mM EDTA, pH 8.0.). The gel was subjected to a voltage of 100 V for 30 min in 0.5 $\times$  TBE running buffer. The gel was then stained by 1 $\times$  SYBR<sup>®</sup> Gold nucleic acid gel stain for 30 min (10  $\mu$ L SYBR<sup>®</sup> Gold stock in 100 mL 1 $\times$  TBE buffer). The stained gel was visualized and recorded by the gel imaging system.

#### **2.3.5. EC Measurements of PG–RCA**

PG–RCA and RCA reactions were performed as described in Section 2.3.5. After the amplification reactions, 10  $\mu$ L of the reaction products were transferred to the ITO electrode chips for DPV measurements (settings are presented in Section 2.3.2).

### **2.3.6. Specificity Test**

The specificity of the new detection scheme was evaluated by using the non-complementary sequence instead of the analyte. Fluorescence and EC measurements were performed. The protocol for PG-RCA with fluorescence measurement was the same as that in Section 2.3.3. The protocol for PG-RCA with EC measurement was the same as that in Section 2.3.4 and Section 2.3.5. The concentration of the non-complementary sequence or the analyte used was 1 nM.

### **2.3.7. Sensitivity Test**

The sensitivity of the new detection scheme was determined by performing a set of experiments with different concentrations of the analyte (0, 100 fM, 1 pM, 10 pM, 100 pM, and 1 nM). The protocol used was the same as that in Section 2.3.4 and Section 2.3.5.

### **2.3.8. Effect of BSA on EC Measurement**

A 20- $\mu$ L solution mixture containing RB, 0.2 mg/mL BSA, and 20  $\mu$ M MB was applied to the ITO electrode chip. DPV measurements were taken every 10 min.

### **2.3.9. Regeneration of the ITO Electrode**

Two methods for the regeneration of the ITO electrode surface were evaluated. After DPV measurement of a PG-RCA reaction product (positive sample with the analyte or

control without the analyte), the ITO electrode surface was rinsed by 20  $\mu\text{L}$  of water for 5 times or sonicated in water for 1 min. The cleaned electrode was then used for repeated measurement of the same reaction product. The regeneration and measurement steps were repeated for 3 more times.

### **2.3.10. EC Detection of PG–RCA at Different Time Points**

To monitor the PG–RCA at different time points of the reaction, 10- $\mu\text{L}$  of the reaction sample was taken out from the reaction tube every 30 min and applied to the ITO electrode chip for EC measurement. The ITO electrode was regenerated between each measurement by water rinsing. The protocol was the same as that in Section 2.3.4 and Section 2.3.5 (analyte concentration of 1 nM).

### **2.3.11. PG–RCA Utilizing Beacon**

To facilitate the formation of the stem–loop structure, the beacon (10 nM in RB) was heated to 94  $^{\circ}\text{C}$  for 10 min, followed by gradual cooling (1  $^{\circ}\text{C}$  per min) to room temperature. The beacon (1 nM final concentration) together with the beacon target (0 or 1 nM) were used to replace the analyte in the PG–RCA reaction mixture. The reaction was allowed to proceed for 1 h. The protocol for PG–RCA utilizing beacon with fluorescence measurement was the same as that in Section 2.3.3. The protocol for PG–RCA utilizing beacon with EC measurement was the same as that in Section 2.3.4 and Section 2.3.5.

## Chapter 3

### Results and Discussion

#### 3.1. EC Detection with Different Electrodes

MB is employed as the redox indicator for the presence of ssDNA in the solution-phase. Therefore, it is important to utilize an electrode that feature a large signal difference between free MB and ssDNA-bound MB. In view of this, three common electrode materials were investigated including gold, Pt, and ITO. The DPV peak currents of ssDNA-bound MB are 24%, 19%, and 66% lower than that of free MB for gold, Pt, and ITO working electrodes, respectively (Figure 3.1 to Figure 3.3). It should be pointed out that the Pt working electrode used was a 2-mm diameter disk electrode sealed in glass (electrode surface 4 times larger than that of the gold and ITO working electrodes). Although the area-normalized peak currents of the ITO electrode are the lowest among the three electrodes, the percentage difference between free MB and ssDNA-bound MB is the largest. The diffusion coefficient of ssDNA-bound MB is smaller than that of free MB. Hence, for all three electrodes, the EC signals from ssDNA-bound MB are lower than that from free MB. For ITO electrode, the electrostatic repulsion between the electrode surface and ssDNA-bound MB contributes further to the signal decrease. These results indicate that MB together with ITO is a good platform for immobilization-free ssDNA detection.

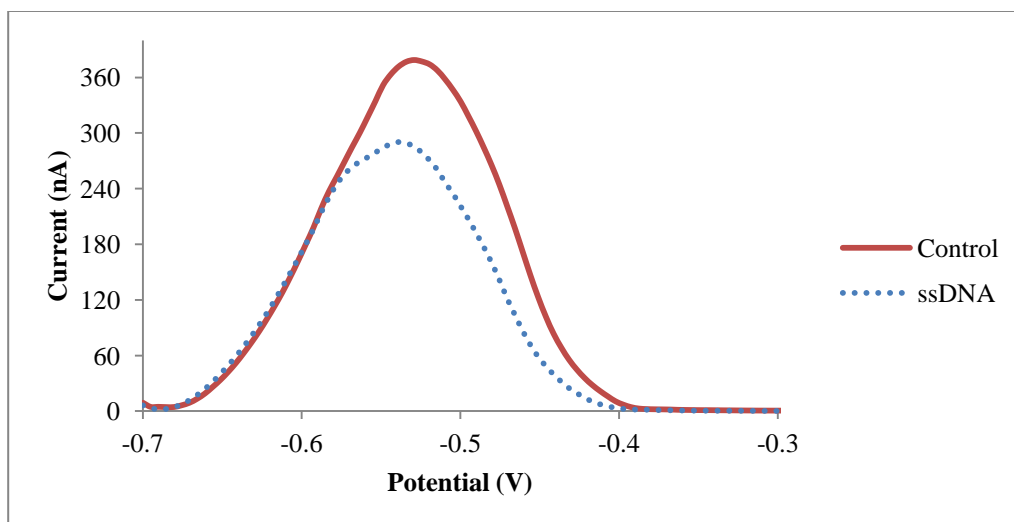


**Figure 3.1.** DPV measurements of MB without and with ssDNA using gold working electrode.

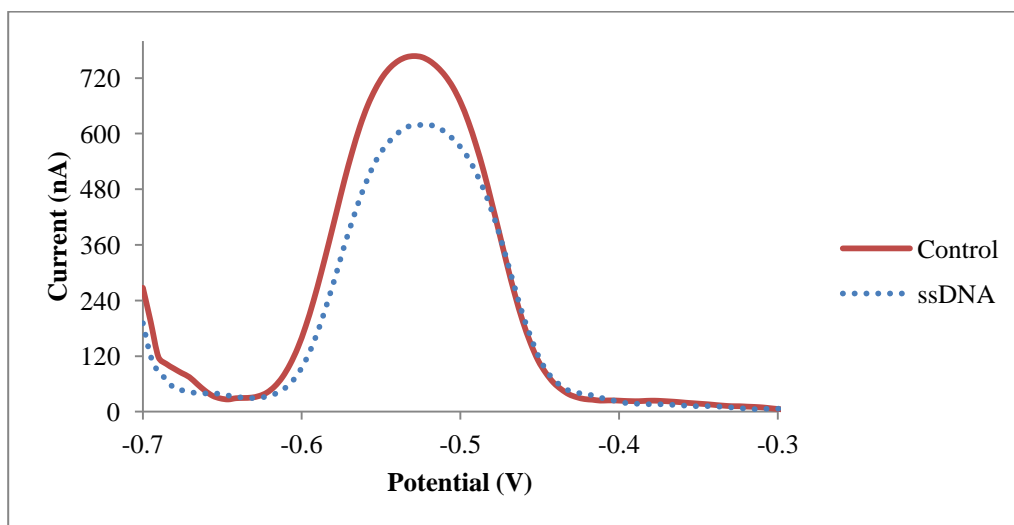


**Figure 3.2.** DPV measurements of MB without and with ssDNA using Pt working electrode.

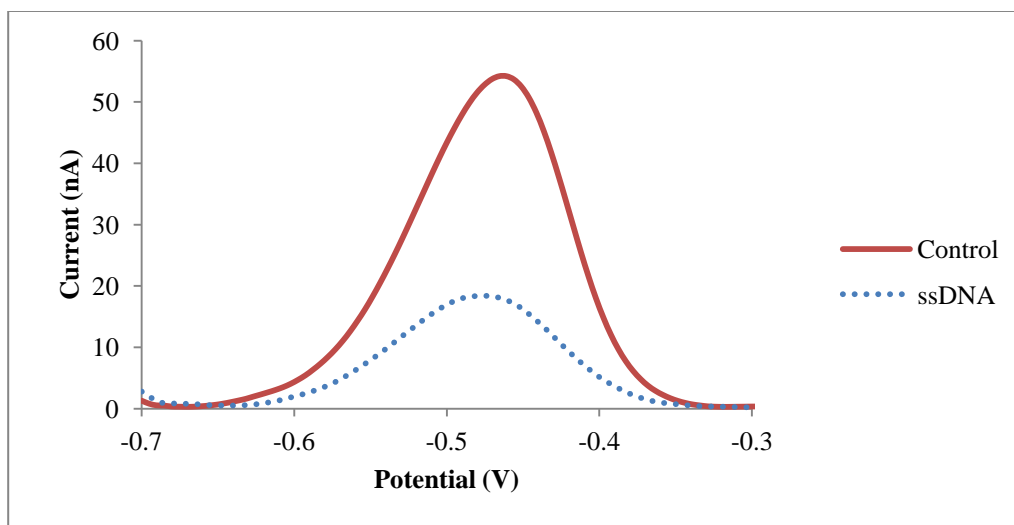


**Figure 3.3.** DPV measurements of MB without and with ssDNA using ITO working electrode.

### 3.2. Effect of MB Concentration on EC ssDNA Detection

The effect of MB concentration on DPV peak current difference between free MB and ssDNA-bound MB was studied (Figure 3.4). The difference in DPV peak currents between free MB and ssDNA-bound MB increases with increasing MB concentration from 1  $\mu\text{M}$  to 20  $\mu\text{M}$ . At 20  $\mu\text{M}$  MB, the difference in DPV peak current reaches a maximum of 66%. At higher MB concentrations, the difference in DPV peak currents decreases with increasing MB concentration. The small signal difference at low MB concentration can be explained by the binding affinity between MB and DNA (dissociation constant in the micromolar range [85]). At low MB concentration, a significant portion of the MB molecules remain free even the ssDNA molecules are in excess. At high MB concentration, since the ssDNA molecules are no longer in excess,

some MB molecules remain free. As a result, at an ssDNA concentration of 10  $\mu\text{M}$ , the optimum MB concentration is 20  $\mu\text{M}$ .

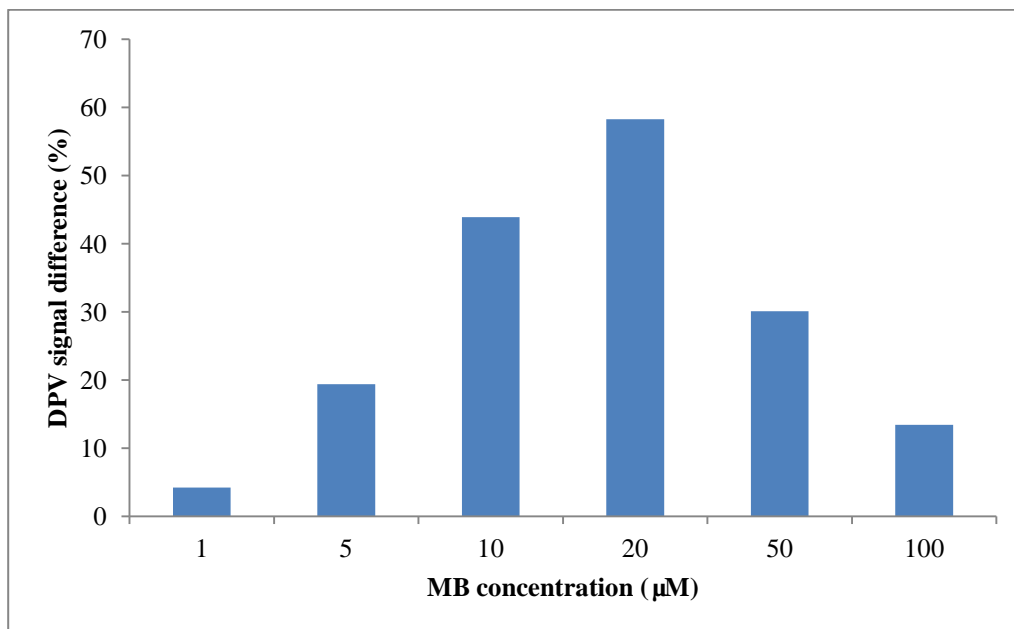


**Figure 3.4.** DPV peak current difference between free MB and ssDNA-bound MB as a function of MB concentration on ITO electrode.

### 3.3. Real-Time Fluorescence Measurement of PG–RCA

Among different isothermal DNA amplification techniques, PG–RCA was utilized in this study. PG–RCA is modified from RCA (which amplifies target sequence in a linear fashion), by the incorporation of a nicking endonuclease, exponential amplification is achieved. Differ from the PG–RCA scheme demonstrated by Komiyama’s group, the PG–RCA reaction was incubated at 37  $^{\circ}\text{C}$  in this work instead of 60  $^{\circ}\text{C}$  [62]. phi29

DNA polymerase and Nb.BbvCI nicking endonuclease, which have optimum activities at 37 °C, were utilized rather than Vent exo<sup>-</sup> polymerase and Nb.BsmI. To validate this new PG-RCA scheme, real-time fluorescence technique was employed. The PG-RCA or RCA reaction is triggered by the presence of the analyte, leading to the generation of ssDNA amplicon. The fluorescent marker, SYBR Gold<sup>®</sup>, binds to the amplicon and thus the fluorescence signal is enhanced. As shown in Figure 3.5, with 1 nM analyte, the fluorescence signal in PG-RCA increased exponentially for the first 90 min and then leveled off afterward. The fluorescence signal of the control (without the analyte) remained flat throughout the 2.5-h reaction. Moreover, the increase in fluorescence signal of PG-RCA is about 18 times PG-RCA larger than that of RCA.

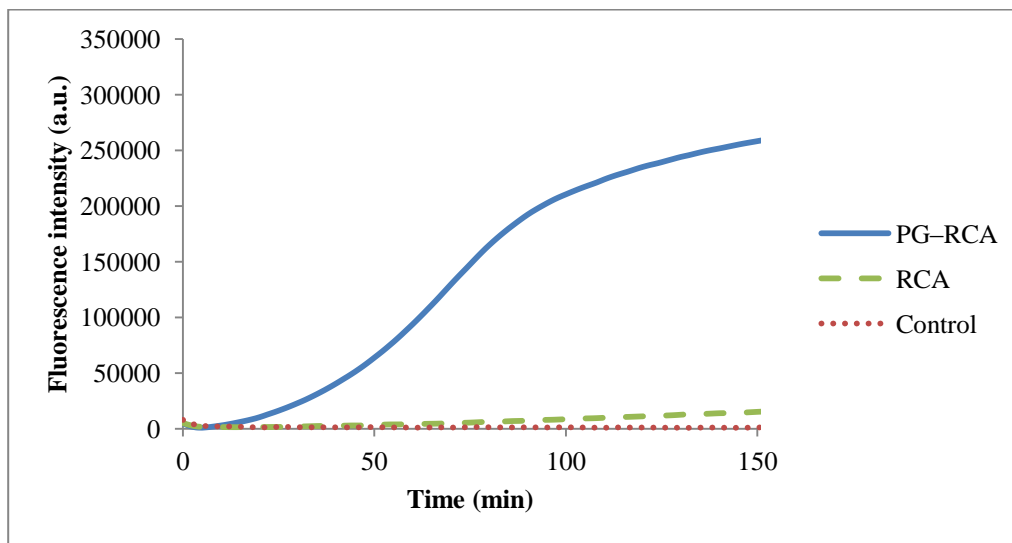


**Figure 3.5.** Real-time fluorescence measurement results of PG-RCA and RCA in the presence of 1 nM analyte; and control (without analyte).

### 3.4. Effect of MB on PG-RCA

It is important to ensure that MB to be compatible with RCA and PG-RCA reactions (i.e., no or negligible inhibition of the enzymatic amplification reactions). Gel electrophoresis analysis was performed to study the compatibility of MB in the RCA and PG-RCA reactions. In order to visualize the RCA products in the gel analysis, 10-fold higher concentration of the analyte (10 nM) was used. RCA and PG-RCA produced ssDNA amplicons of different lengths and thus smearing was observed in the gel results (Figure 3.6, lanes 5–8). The similar gel results in cases without and with MB for RCA (lane 5 and lane 6, respectively) as well as for PG-RCA (lane 7 and lane 8, respectively) confirm that the presence of 20  $\mu$ M MB has negligible inhibitory effect on the amplification results.

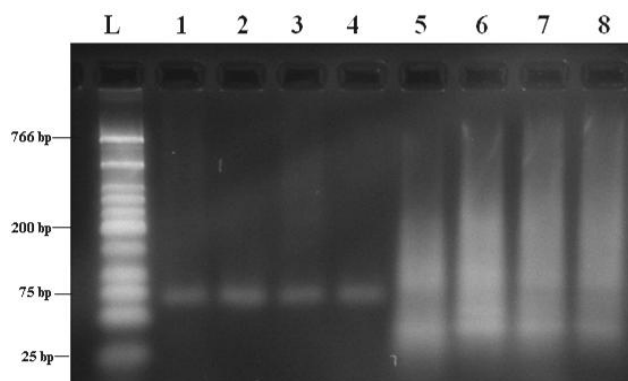


**Figure 3.6.** Agarose gel electrophoresis results showing the effects of MB on PG-RCA and RCA. Lane L: DNA ladder; lanes 1, 3, 5, and 7: without MB; lanes 2, 4, 6, and 8: with 20  $\mu$ M MB; lanes 5 and 6: RCA with 10 nM analyte; lanes 7 and 8: PG-RCA with 1 nM analyte; lanes 1–4: control reactions (without analyte) for lanes 5–8.

### 3.5. EC Measurements of PG-RCA

The reaction products of PG-RCA and RCA with 20  $\mu\text{M}$  MB and 1 nM analyte were measured by DPV (Figure 3.7). For PG-RCA, the DPV peak current dropped from 52.4 nA (without analyte) to 18.4 nA (with analyte), i.e., a 65% decrease in the EC signal. This is consistent with the results with synthetic ssDNA (10  $\mu\text{M}$ ) as described in Section 3.1 (Figure 3.3). For RCA, the DPV peak current dropped from 52.4 nA (without analyte) to 49.6 nA (with analyte), i.e., a 5% decrease in the EC signal. Therefore, PG-RCA results in a signal change 13-fold larger than RCA, which is similar to that obtained by the real-time fluorescence technique as described in Section 3.3 (Figure 3.5).

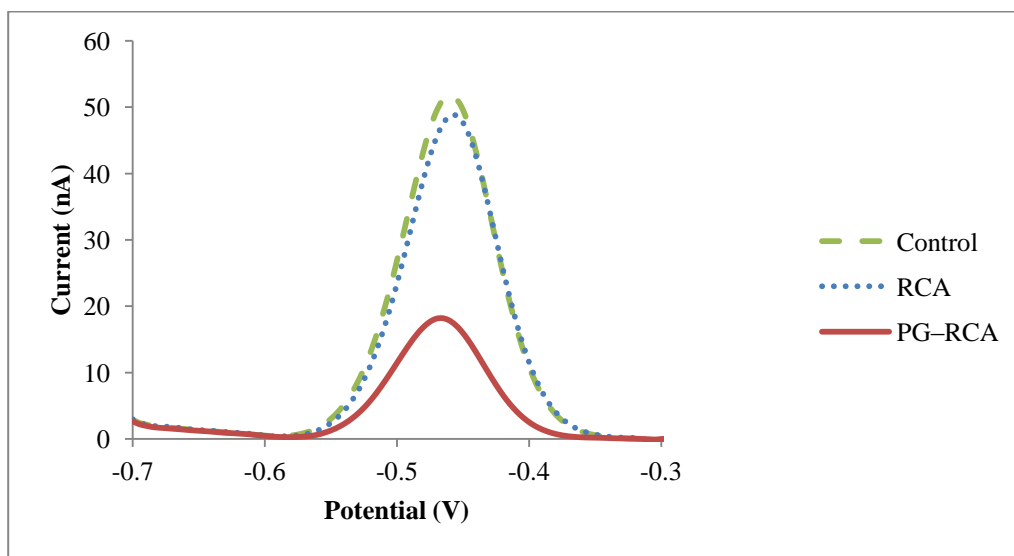


**Figure 3.7.** EC detection results of PG-RCA and RCA in the presence of 1 nM analyte; and control (without analyte).

### 3.6. Specificity Test

The specificity of the new detection sequence was evaluated by replacing the analyte with the non-complementary sequence. The performance was first evaluated by real-time fluorescence measurements. As expected, the fluorescence signal of the non-complementary sequence sample was similar to that of the control (no analyte) (Figure 3.8). Then, EC measurements were also carried out (Figure 3.9). The DPV signal of the non-complementary sequence sample was almost identical to that of the control (no analyte).

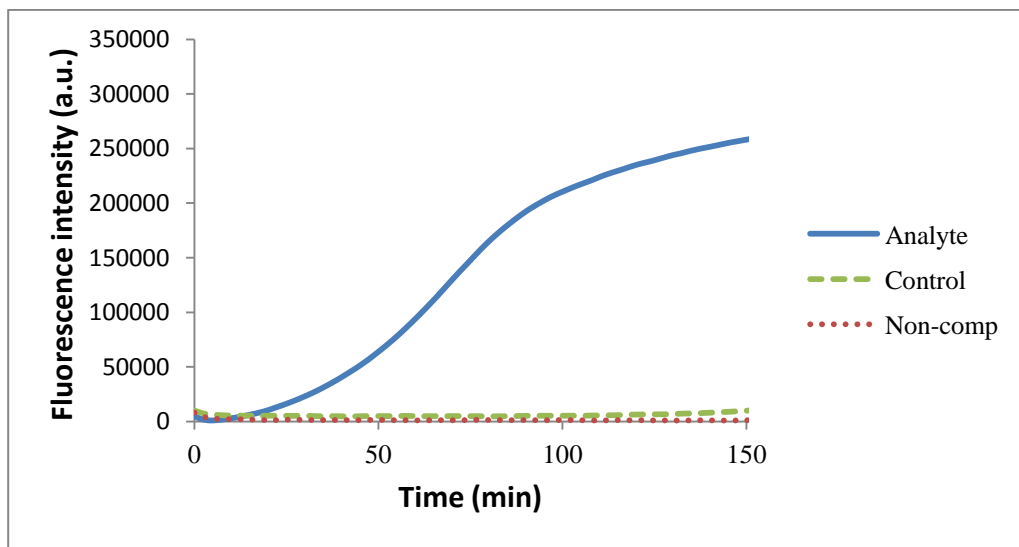


**Figure 3.8.** Real-time fluorescence measurement results of PG–RCA with the analyte, non-complementary sequence (non-comp), and control (no analyte).

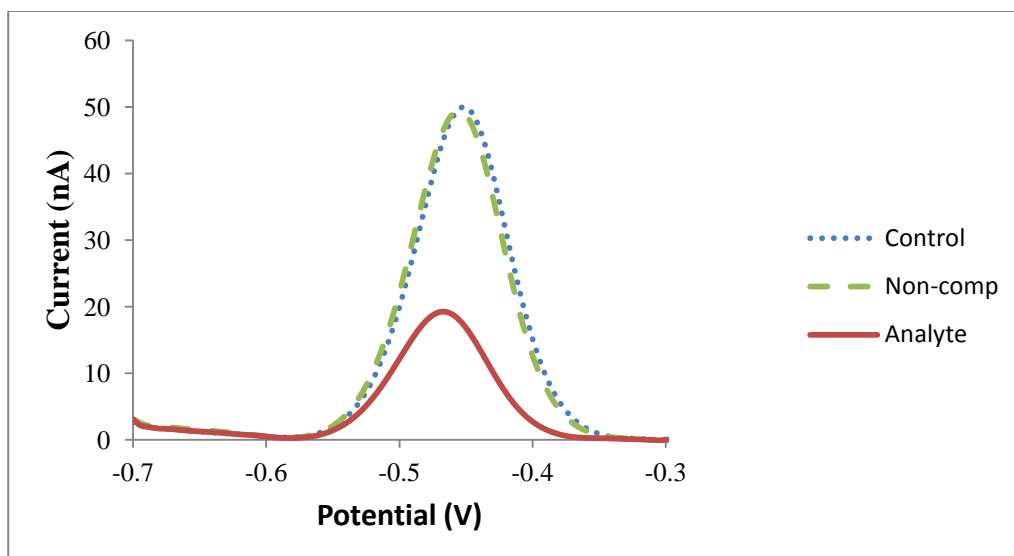


**Figure 3.9.** EC detection results of PG-RCA with the analyte, non-complementary sequence (non-comp), and control (no analyte).

### 3.7. Sensitivity Test

Figure 3.10 shows the real-time fluorescence signals of PG-RCA with different analyte concentrations (a 10-fold serial dilution from 1 nM to 1 pM). The fluorescence signal of the sample with 1 pM analyte is slightly above that of the control (without analyte). End-point EC measurements of PG-RCA with different analyte concentrations (a 10-fold serial dilution from 1 nM to 100 fM) were also performed (Figure 3.11). The DPV peak current decreases with increasing analyte concentration. When the DPV peak current is plotted against logarithm of analyte concentration, a linear relationship is obtained (Figure 3.12). The detection limit of this EC detection scheme is 100 fM (based on mean of the control  $\pm 3SD$ ).

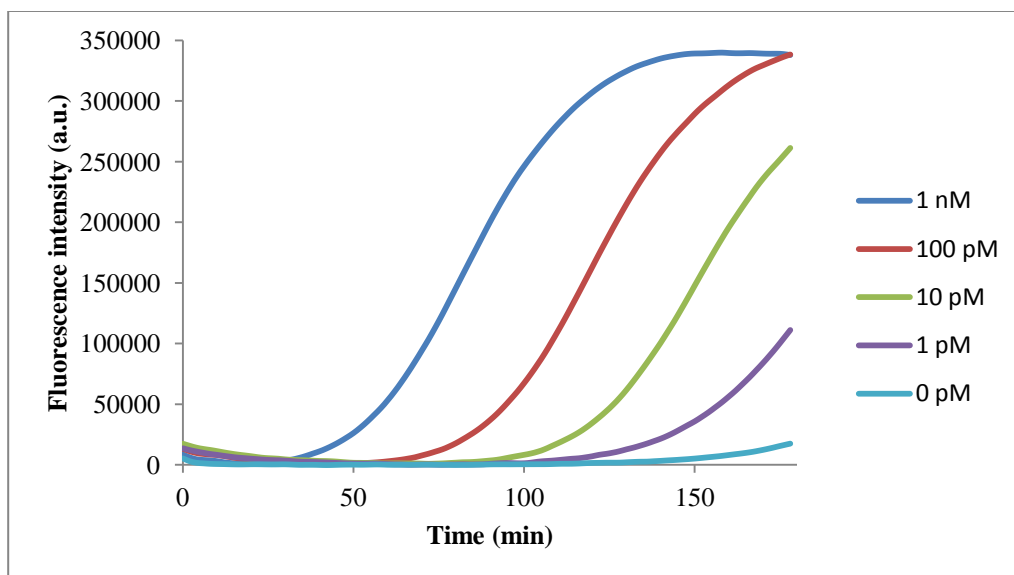


**Figure 3.10.** Real-time fluorescence measurement results of PG-RCA with different concentrations of analyte.

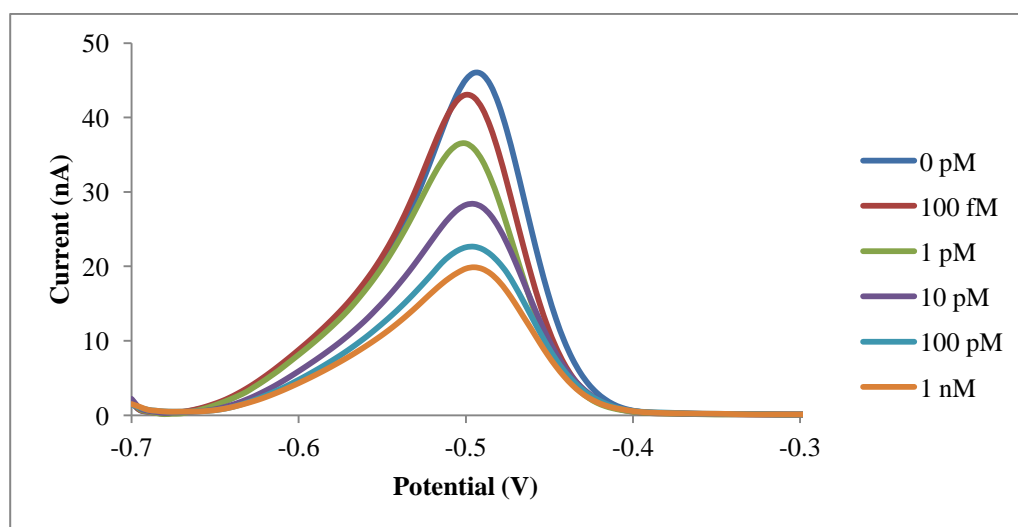


**Figure 3.11.** EC detection results of PG-RCA with different concentrations of analyte.

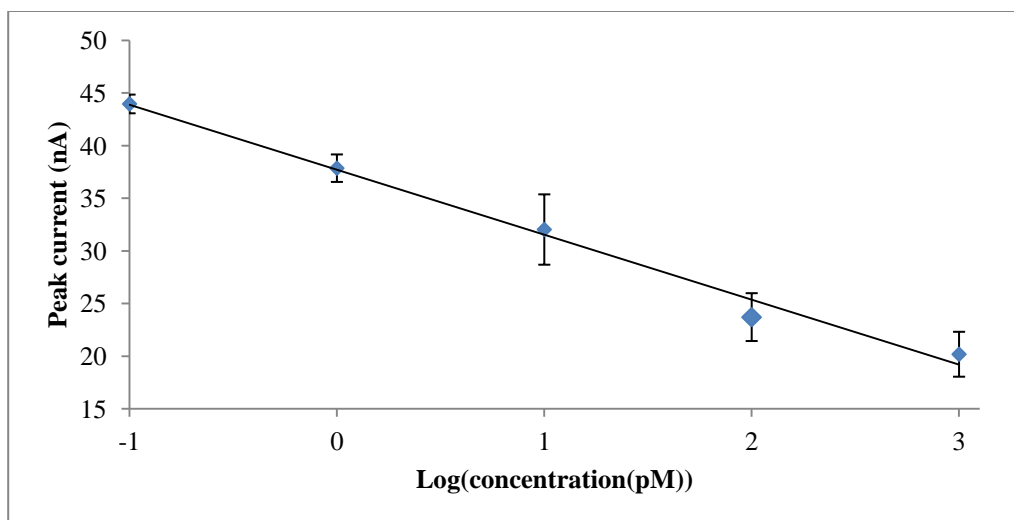


**Figure 3.12.** Plot of peak current against logarithm of analyte concentration with constant MB concentration.

### 3.8. Absorption on ITO Electrode

Electrode fouling is a common issue associated with EC measurement of complex sample matrix such as enzymatic reaction mixture. The non-specific adsorption of protein molecules is a major contributor to electrode fouling. The adsorption effect of BSA on MB redox signal was studied. As shown in Figure 3.13, the DPV peak current decreases with increasing incubation time. After 60-min incubation, the DPV peak current dropped to 53% of the initial value. This can be explained by the fact that the adsorbed BSA hinders the MB molecules from approaching the electrode surface. This result implies that real-time measurement of PG-RCA with a single electrode would be difficult without a surface regeneration step.

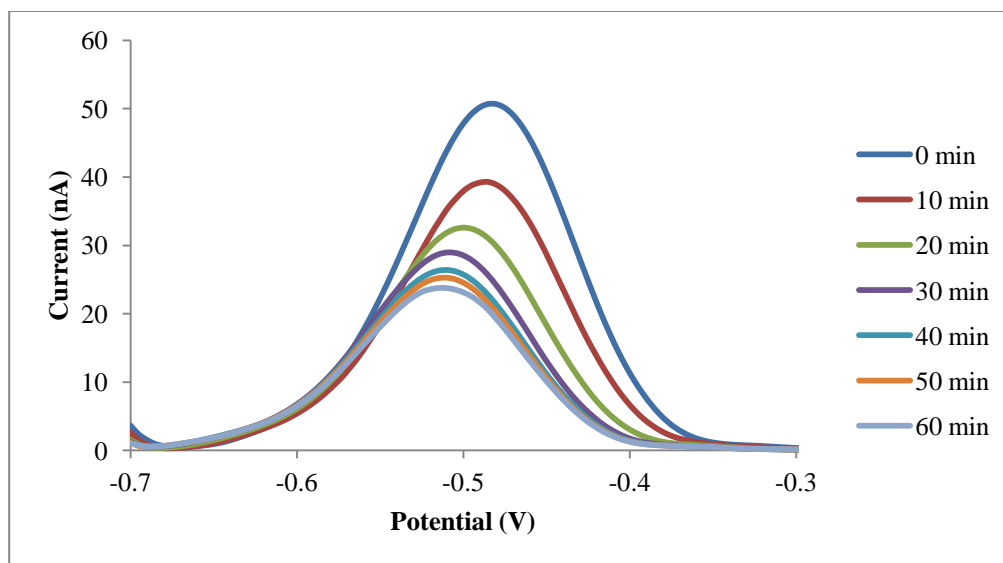


**Figure 3.13.** EC measurements of MB in solution containing BSA at different time points.

### 3.9. Regeneration of ITO Electrode Surface

Two electrode surface regeneration methods were investigated including simple rinsing with water and sonication in water. The same sample (control without analyte or positive sample with analyte) was measured 5 times with a regeneration step in between. For simple rinsing with water, the EC signals of the control and positive samples at the fifth measurement are only slightly lower (< 10%) than that at the first measurement (Figure 3.14). For sonication in water, the EC signals remain unchanged (Figure 3.15). These data suggest that the non-specific adsorption on the ITO electrode is not permanent and can be regenerated easily.

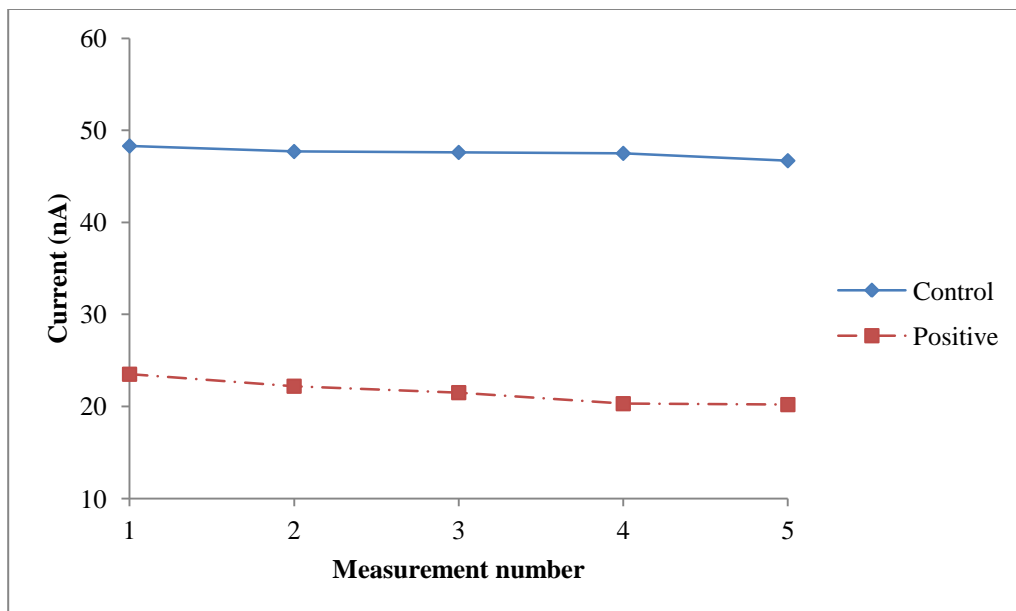


**Figure 3.14.** Regeneration of ITO electrode surface by water rinsing.

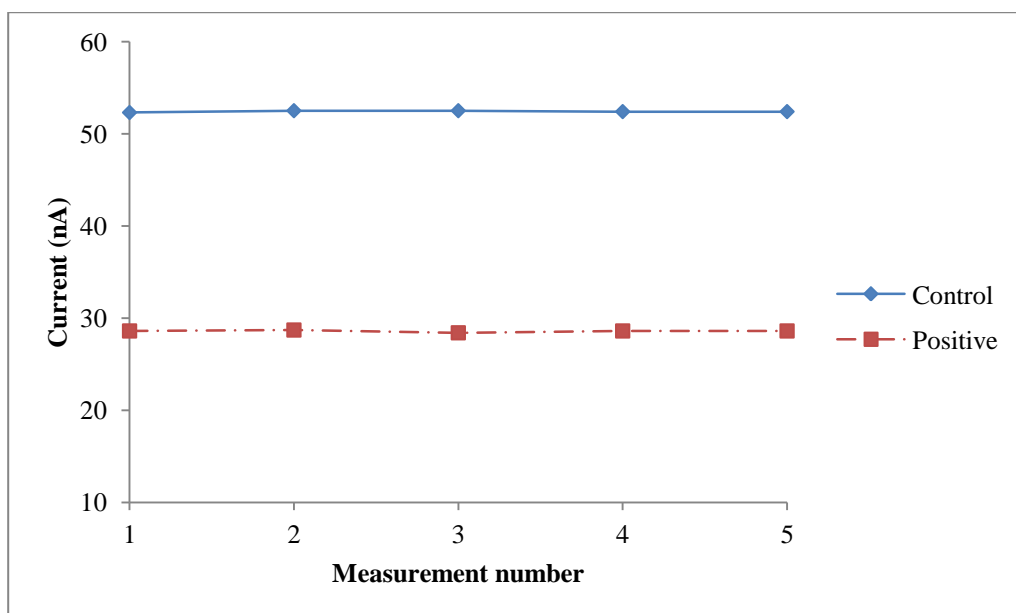


**Figure 3.15.** Regeneration of ITO electrode surface by sonication in water.

### 3.10. EC Detection of PG–RCA at Different Time Points

Attempt was made to monitor the EC signal in course of the PG–RCA reaction. EC measurements were performed every 30 min by pipetting a 10- $\mu$ L sample (control without analyte or positive sample with analyte) out from the reaction tube and transferring it to the ITO electrode chip. A simple water rinsing electrode surface regeneration step was carried out after each measurement. As shown in Figure 3.16, the positive sample features an exponential decrease in the EC signal for the first 90 min and levels off afterward. This profile is similar to that of the real-time fluorescence measurement (Figure 3.5), except the latter one having signal increase instead.

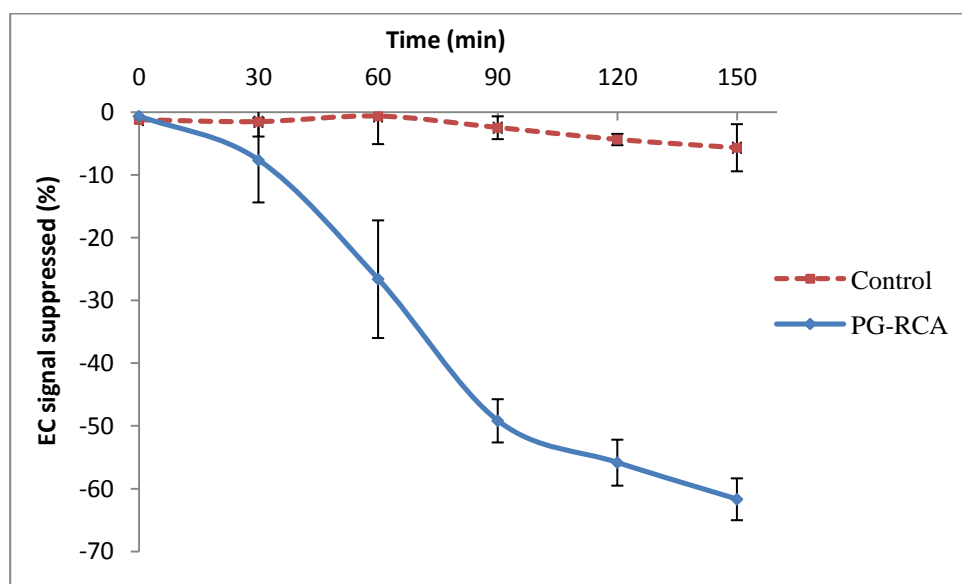


**Figure 3.16.** Plot of DPV signal change as a function of PG–RCA reaction time.

### 3.11. PG–RCA using DNA Beacon

To allow the detection of target sequence not located at the 3'-end, a molecular beacon recognition probe was employed. Upon the hybridization of the complementary beacon target sequence to the beacon, the 3'-end of the beacon then hybridizes with the circular template and PG–RCA is initiated. Both real-time fluorescence and EC measurements prove that the beacon allows internal target sequence to be detected (Figure 3.17 and Figure 3.18). It should be noted that, to prevent false initiation of the PG–RCA reaction, the melting temperature of the stem should be higher than that of the 3'-end stem–circular template hybrid.

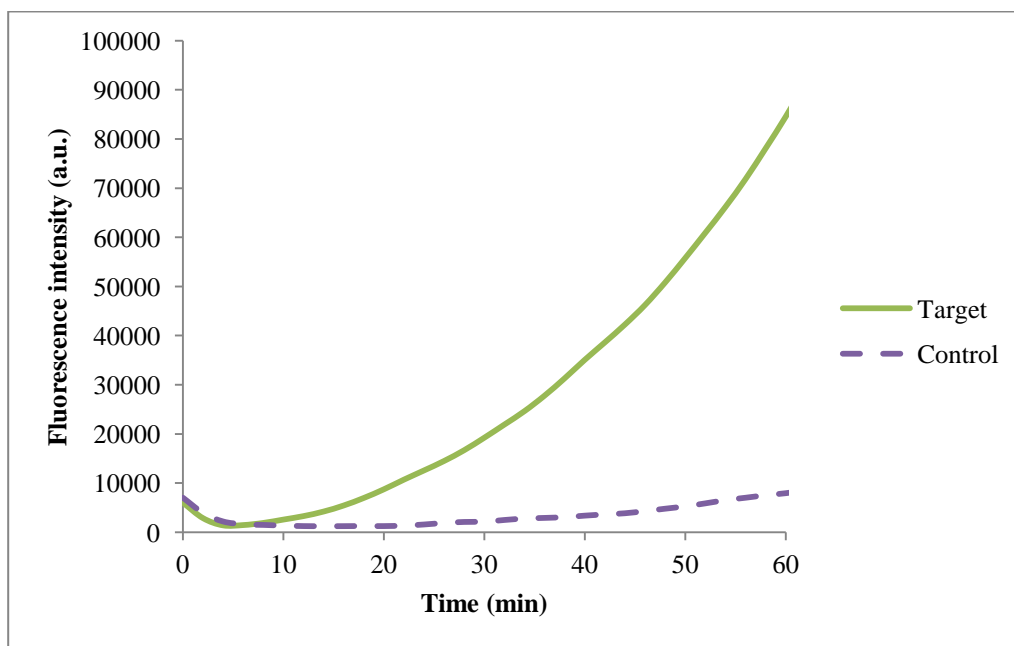


**Figure 3.17.** Real-time fluorescence measurement results of PG–RCA utilizing beacon.

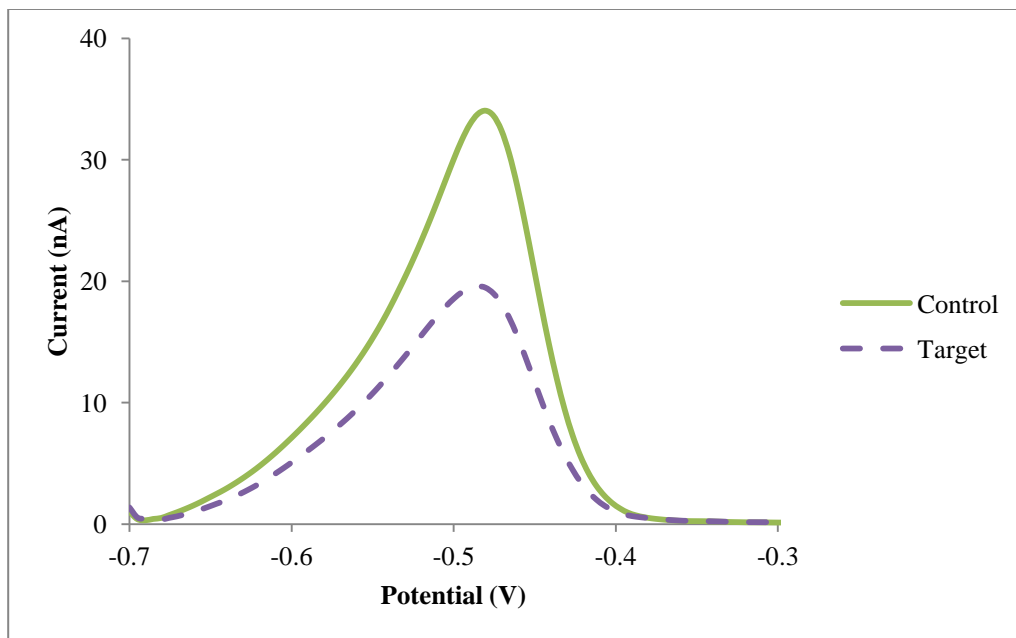


**Figure 3.18.** EC measurement results of PG-RCA utilizing beacon.

## Chapter 4

### Conclusions and Recommendations for Future Work

#### 4.1. Key Findings and Conclusions

In this study, a simple and sensitive EC DNA sensor was developed. MB redox indicator and ITO working electrode were successfully employed to detect ssDNA in an immobilization-free format. PG-RCA was utilized to achieve isothermal exponential DNA amplification. phi29 DNA polymerase and Nb.BbvCI nicking endonuclease with 37 °C optimum operating temperature were employed in the reaction. With 10 μM ssDNA, the optimum MB concentration was 20 μM. Real-time fluorescence measurement and the gel electrophoresis analysis were utilized as alternative tools to study the performance of the enzymatic reaction. All of the results from EC detection, fluorescence measurement, and gel electrophoresis showed that PG-RCA offers much higher sensitivity than RCA. Moreover, the result from gel electrophoresis showed that MB is compatible in the enzymatic reaction. The specificity was studied using non-complementary sequence. Results showed that the PG-RCA scheme offered specific detection. The detection limit of the new detection scheme was 100 fM, which was comparable to fluorescence method with SYBR<sup>®</sup> Gold. The linear working range was from 100 fM to 1 nM. Electrode fouling was found to be attributed to the non-specific protein adsorption. The electrode surface can be regenerated by simple rinsing with water or sonication in water. EC measurements of the PG-RCA reaction products at

different time points using a single electrode chip with regeneration step showed a consistent reaction profile with the real-time fluorescence measurement. Furthermore, molecular beacon was successfully utilized to detect internal target sequence. To conclude, the simplicity of the new detection scheme, which includes primer design, electrode preparation, and instrumentation, is conducive to decentralized DNA analysis.

## **4.2. Recommendations for Future Work**

Based on the new detection scheme developed in this study, several further investigations can be carried out. First, the sensitivity should be further enhanced. This can be achieved by optimizing the PG-RCA protocol such as sequence design, enzyme, and operating temperature. Utilizing different isothermal DNA amplification strategies may also be possible to achieve higher sensitivity. The analysis of real-life sample should be investigated.

Second, the bare ITO electrode cannot be used for real-time monitoring due to the non-specific adsorption of protein molecules onto the electrode surface. To address this issue, an anti-fouling coating (e.g., polyethylene glycol) is needed to passivate the electrode surface. The use of other electrode materials (e.g., carbon) as well as types of electrodes (e.g., low-cost screen-printed electrodes) should be explored.

Last but not least, in addition to DNA, the target analytes of this sensing platform can be extended to protein and small molecule. Indeed, a number of previous reports demonstrated protein and small molecule detection coupled to isothermal DNA amplification [86-91]. One key element is to incorporate antibody or aptamer [92-93] recognition moiety into the target-triggered isothermal amplification scheme.

## References

- [1] Ramsay, G. DNA chips: State-of-the art. *Nat. Biotechnol.* **16**, 40–44 (1998).
- [2] Tyagi, S. & Kramer, F. R. Molecular beacons: Probes that fluoresce upon hybridization. *Nat. Biotechnol.* **14**, 303–308 (1996).
- [3] Heid, C. A., Stevens, J., Livak, K. J. & Williams, P. M. Real time quantitative PCR. *Genome Res.* **6**, 986–994 (1996).
- [4] Bustin, S. Absolute quantification of mRNA using real-time reverse transcription polymerase chain reaction assays. *J. Mol. Endocrinol.* **25**, 169–193 (2000).
- [5] Luo, X. & Hsing, I.-M. Electrochemical techniques on sequence-specific PCR amplicon detection for point-of-care applications. *Analyst* **134**, 1957–1964 (2009).
- [6] Wang, J. Electrochemical nucleic acid biosensors. *Anal. Chim. Acta* **469**, 63–71 (2002).
- [7] Drummond, T. G., Hill, M. G. & Barton, J. K. Electrochemical DNA sensors. *Nat. Biotechnol.* **21**, 1192–1199 (2003).
- [8] Paleček, E. & Bartošík, M. Electrochemistry of nucleic acids. *Chem. Rev.* **112**, 3427–3481 (2012).
- [9] Millan, K. M. & Mikkelsen, S. R. Sequence-selective biosensor for DNA based on electroactive hybridization indicators. *Anal. Chem.* **65**, 2317–2323 (1993).
- [10] Watson, J., D. & Crick, F., H., C. Molecular structure of nucleic acids. *Nature* **171**, 737–738 (1953).
- [11] Hashimoto, K., Ito, K. & Ishimori, Y. Sequence-specific gene detection with a gold electrode modified with DNA probes and an electrochemically active dye. *Anal. Chem.* **66**, 3830–3833 (1994).

- [12] Steel, A. B., Herne, T. M. & Tarlov, M. J. Electrochemical quantitation of DNA immobilized on gold. *Anal. Chem.* **70**, 4670–4677 (1998).
- [13] Kelley, S. O., Boon, E. M., Barton, J. K., Jackson, N. M. & Hill, M. G. Single-base mismatch detection based on charge transduction through DNA. *Nucleic Acids Res.* **27**, 4830–4837 (1999).
- [14] Cheng, A. K. H., Ge, B. & Yu, H.-Z. Aptamer-based biosensors for label-free voltammetric detection of lysozyme. *Anal. Chem.* **79**, 5158–5164 (2007).
- [15] Umek, R. M., Lin, S. W., Vielmetter, J., Terbrueggen, R. H., Irvine, B., Yu, C. J., Kayyem, J. F., Yowanto, H., Blackburn, G. F., Farkas, D. H. & Chen, Y.-P. Electronic detection of nucleic acids: A versatile platform for molecular diagnostics. *J. Mol. Diagn.* **3**, 74–84 (2001).
- [16] Fan, C., Plaxco, K. W. & Heeger, A. J. Electrochemical interrogation of conformational changes as a reagentless method for the sequence-specific detection of DNA. *Proc. Natl. Acad. Sci. U. S. A.* **100**, 9134–9137 (2003).
- [17] Xiao, Y., Lubin, A. A., Baker, B. R., Plaxco, K. W. & Heeger, A. J. Single-step electronic detection of femtomolar DNA by target-induced strand displacement in an electrode-bound duplex. *Proc. Natl. Acad. Sci. U. S. A.* **103**, 16677–16680 (2006).
- [18] Xiao, Y., Qu, X., Plaxco, K. W. & Heeger, A. J. Label-free electrochemical detection of DNA in blood serum via target-induced resolution of an electrode-bound DNA pseudoknot. *J. Am. Chem. Soc.* **129**, 11896–11897 (2007).
- [19] Patolsky, F., Katz, E., Bardea, A. & Willner, I. Enzyme-linked amplified electrochemical sensing of oligonucleotide–DNA interactions by means of the

- precipitation of an insoluble product and using impedance spectroscopy. *Langmuir* **15**, 3703–3706 (1999).
- [20] Campbell, C. N., Gal, D., Cristler, N., Banditrat, C. & Heller, A. Enzyme-amplified amperometric sandwich test for RNA and DNA. *Anal. Chem.* **74**, 158–162 (2001).
- [21] Authier, L., Grossiord, C., Brossier, P. & Limoges, B. Gold nanoparticle-based quantitative electrochemical detection of amplified human cytomegalovirus DNA using disposable microband electrodes. *Anal. Chem.* **73**, 4450–4456 (2001).
- [22] Ozsoz, M., Erdem, A., Kerman, K., Ozkan, D., Tugrul, B., Topcuoglu, N., Ekren, H. & Taylan, M. Electrochemical genosensor based on colloidal gold nanoparticles for the detection of factor V Leiden mutation using disposable pencil graphite electrodes. *Anal. Chem.* **75**, 2181–2187 (2003).
- [23] Zhang, J., Song, S., Wang, L., Pan, D. & Fan, C. A gold nanoparticle-based chronocoulometric DNA sensor for amplified detection of DNA. *Nat. Protoc.* **2**, 2888–2895 (2007).
- [24] Wang, J., Rivas, G., Fernandes, J. R., Lopez Paz, J. L., Jiang, M. & Waymire, R. Indicator-free electrochemical DNA hybridization biosensor. *Anal. Chim. Acta* **375**, 197–203 (1998).
- [25] Kerman, K., Morita, Y., Takamura, Y. & Tamiya, E. Label-free electrochemical detection of DNA hybridization on gold electrode. *Electrochem. Commun.* **5**, 887–891 (2003).
- [26] Korri-Youssoufi, H., Garnier, F., Srivastava, P., Godillot, P. & Yassar, A. Toward bioelectronics: Specific DNA recognition based on an oligonucleotide-functionalized polypyrrole. *J. Am. Chem. Soc.* **119**, 7388–7389 (1997).

- [27] Fritz, J., Cooper, E. B., Gaudet, S., Sorger, P. K. & Manalis, S. R. Electronic detection of DNA by its intrinsic molecular charge. *Proc. Natl. Acad. Sci. U. S. A.* **99**, 14142–14146 (2002).
- [28] Hahm, J.-i. & Lieber, C. M. Direct ultrasensitive electrical detection of DNA and DNA sequence variations using nanowire nanosensors. *Nano Lett.* **4**, 51–54 (2003).
- [29] Sassolas, A., Leca-Bouvier, B. D. & Blum, L. J. DNA biosensors and microarrays. *Chem. Rev.* **108**, 109–139 (2007).
- [30] Osborne, S. E., Vdker, J., Stevens, S. Y., Breslauer, K. J. & Glick, G. D. Design, synthesis, and analysis of disulfide cross-linked DNA duplexes. *J. Am. Chem. Soc.* **118**, 11993–12003 (1996).
- [31] Lee, C.-Y., Canavan, H. E., Gamble, L. J. & Castner, D. G. Evidence of impurities in thiolated single-stranded DNA oligomers and their effect on DNA self-assembly on gold. *Langmuir* **21**, 5134–5141 (2005).
- [32] Marrazza, G., Chianella, I. & Mascini, M. Disposable DNA electrochemical sensor for hybridization detection. *Biosens. Bioelectron.* **14**, 43–51 (1999).
- [33] Napier, M. E. & Thorp, H. H. Modification of electrodes with dicarboxylate self-assembled monolayers for attachment and detection of nucleic acids. *Langmuir* **13**, 6342–6344 (1997).
- [34] Lee, T. M.-H., Li, L.-L. & Hsing, I. M. Enhanced electrochemical detection of DNA hybridization based on electrode-surface modification. *Langmuir* **19**, 4338–4343 (2003).
- [35] Eckhardt, A. E., Mikulecky, J. C., Napier, M. E., Thomas, R. S. & Thorp, H. H. Monolayer and electrode for detection a label-bearing target and method of use thereof. *U.S. Patent*, 6 127 127 (2000).

- [36] Lee, T. M.-H., Carles, M. C. & Hsing, I. M. Microfabricated PCR-electrochemical device for simultaneous DNA amplification and detection. *Lab Chip* **3**, 100–105 (2003).
- [37] Li, L.-L., Cai, H., Lee, T. M.-H., Barford, J. & Hsing, I. M. Electrochemical detection of PCR amplicons using electroconductive polymer modified electrode and multiple nanoparticle labels. *Electroanalysis* **16**, 81–87 (2004).
- [38] Yeung, S.-W., Lee, T. M.-H., Cai, H. & Hsing, I.-M. A DNA biochip for on-the-spot multiplexed pathogen identification. *Nucleic Acids Res.* **34**, e118 (2006).
- [39] Ricci, F., Lai, R. Y., Heeger, A. J., Plaxco, K. W. & Sumner, J. J. Effect of molecular crowding on the response of an electrochemical DNA sensor. *Langmuir* **23**, 6827–6834 (2007).
- [40] Lubin, A. A. & Plaxco, K. W. Folding-based electrochemical biosensors: The case for responsive nucleic acid architectures. *Acc. Chem. Res.* **43**, 496–505 (2010).
- [41] Lao, R., Song, S., Wu, H., Wang, L., Zhang, Z., He, L. & Fan, C. Electrochemical interrogation of DNA monolayers on gold surfaces. *Anal. Chem.* **77**, 6475–6480 (2005).
- [42] Herne, T. M. & Tarlov, M. J. Characterization of DNA probes immobilized on gold surfaces. *J. Am. Chem. Soc.* **119**, 8916–8920 (1997).
- [43] Kobayashi, M., Kusakawa, T., Saito, M., Kaji, S., Oomura, M., Iwabuchi, S., Morita, Y., Hasan, Q. & Tamiya, E. Electrochemical DNA quantification based on aggregation induced by Hoechst 33258. *Electrochem. Commun.* **6**, 337–343 (2004).
- [44] Luo, X., Lee, T. M.-H. & Hsing, I. M. Immobilization-free sequence-specific electrochemical detection of DNA using ferrocene-labeled peptide nucleic acid. *Anal. Chem.* **80**, 7341–7346 (2008).

- [45] Egholm, M., Buchardt, O., Christensen, L., Behrens, C., Freier, S. M., Driver, D. A., Berg, R. H., Kim, S. K., Norden, B. & Nielsen, P. E. PNA hybridizes to complementary oligonucleotides obeying the Watson–Crick hydrogen-bonding rules. *Nature* **365**, 566–568 (1993).
- [46] Saiki, R., Gelfand, D., Stoffel, S., Scharf, S., Higuchi, R., Horn, G., Mullis, K. & Erlich, H. Primer-directed enzymatic amplification of DNA with a thermostable DNA polymerase. *Science* **239**, 487–491 (1988).
- [47] Ririe, K. M., Rasmussen, R. P. & Wittwer, C. T. Product differentiation by analysis of DNA melting curves during the polymerase chain reaction. *Anal. Biochem.* **245**, 154–160 (1997).
- [48] Liu, R. H., Yang, J., Lenigk, R., Bonanno, J. & Grodzinski, P. Self-contained, fully integrated biochip for sample preparation, polymerase chain reaction amplification, and DNA microarray detection. *Anal. Chem.* **76**, 1824–1831 (2004).
- [49] Yeung, S. S. W., Lee, T. M. H. & Hsing, I. M. Electrochemical real-time polymerase chain reaction. *J. Am. Chem. Soc.* **128**, 13374–13375 (2006).
- [50] Yeung, S. S. W., Lee, T. M. H. & Hsing, I. M. Electrochemistry-based real-time PCR on a microchip. *Anal. Chem.* **80**, 363–368 (2007).
- [51] Ahmed, M. U., Idegami, K., Chikae, M., Kerman, K., Chaumpluk, P., Yamamura, S. & Tamiya, E. Electrochemical DNA biosensor using a disposable electrochemical printed (DEP) chip for the detection of SNPs from unpurified PCR amplicons. *Analyst* **132**, 431–438 (2007).

- [52] Fang, T. H., Ramalingam, N., Xian-Dui, D., Ngin, T. S., Xianting, Z., Lai Kuan, A. T., Peng Huat, E. Y. & Hai-Qing, G. Real-time PCR microfluidic devices with concurrent electrochemical detection. *Biosens. Bioelectron.* **24**, 2131–2136 (2009).
- [53] Defever, T., Druet, M., Rochelet-Dequaire, M., Joannes, M., Grossiord, C., Limoges, B. & Marchal, D. Real-time electrochemical monitoring of the polymerase chain reaction by mediated redox catalysis. *J. Am. Chem. Soc.* **131**, 11433–11441 (2009).
- [54] Deféver, T., Druet, M., Evrard, D., Marchal, D. & Limoges, B. Real-time electrochemical PCR with a DNA intercalating redox probe. *Anal. Chem.* **83**, 1815–1821 (2011).
- [55] Luo, X., Xuan, F. & Hsing, I. M. Real time electrochemical monitoring of PCR amplicons using electroactive hydrolysis probe. *Electrochem. Commun.* **13**, 742–745 (2011).
- [56] Walker, G. T., Fraiser, M. S., Schram, J. L., Little, M. C., Nadeau, J. G. & Malinowski, D. P. Strand displacement amplification—an isothermal, in vitro DNA amplification technique. *Nucleic Acids Res.* **20**, 1691–1696 (1992).
- [57] Fire, A. & Xu, S. Q. Rolling replication of short DNA circles. *Proc. Natl. Acad. Sci. U. S. A.* **92**, 4641–4645 (1995).
- [58] Liu, D., Daubendiek, S. L., Zillman, M. A., Ryan, K. & Kool, E. T. Rolling circle DNA synthesis: Small circular oligonucleotides as efficient templates for DNA polymerases. *J. Am. Chem. Soc.* **118**, 1587–1594 (1996).
- [59] Notomi, T., Okayama, H., Masubuchi, H., Yonekawa, T., Watanabe, K., Amino, N. & Hase, T. Loop-mediated isothermal amplification of DNA. *Nucleic Acids Res.* **28**, e63 (2000).

- [60] Vincent, M., Xu, Y. & Kong, H. Helicase-dependent isothermal DNA amplification. *EMBO Rep.* **5**, 795–800 (2004).
- [61] Guo, Q., Yang, X., Wang, K., Tan, W., Li, W., Tang, H. & Li, H. Sensitive fluorescence detection of nucleic acids based on isothermal circular strand-displacement polymerization reaction. *Nucleic Acids Res.* **37**, e20 (2009).
- [62] Murakami, T., Sumaoka, J. & Komiyama, M. Sensitive isothermal detection of nucleic acid sequence by primer generation–rolling circle amplification. *Nucleic Acids Res.* **37**, e19 (2009).
- [63] Li, J. J., Chu, Y., Lee, B. Y.-H. & Xie, X. S. Enzymatic signal amplification of molecular beacons for sensitive DNA detection. *Nucleic Acids Res.* **36**, e36 (2008).
- [64] Xu, W., Xue, X., Li, T., Zeng, H. & Liu, X. Ultrasensitive and selective colorimetric DNA detection by nicking endonuclease assisted nanoparticle amplification. *Angew. Chem., Int. Ed.* **48**, 6849–6852 (2009).
- [65] Cui, L., Ke, G., Wang, C. & Yang, C. J. A cyclic enzymatic amplification method for sensitive and selective detection of nucleic acids. *Analyst* **135**, 2069–2073 (2010).
- [66] Hsieh, K., Xiao, Y. & Tom Soh, H. Electrochemical DNA detection via exonuclease and target-catalyzed transformation of surface-bound probes. *Langmuir* **26**, 10392–10396 (2010).
- [67] Lee, H. J., Li, Y., Wark, A. W. & Corn, R. M. Enzymatically amplified surface plasmon resonance imaging detection of DNA by exonuclease III digestion of DNA microarrays. *Anal. Chem.* **77**, 5096–5100 (2005).

- [68] Zhao, W. A., Ali, M. M., Brook, M. A. & Li, Y. F. Rolling circle amplification: Applications in nanotechnology and biodetection with functional nucleic acids. *Angew. Chem., Int. Ed.* **47**, 6330–6337 (2008).
- [69] Lizardi, P. M., Huang, X. H., Zhu, Z. R., Bray-Ward, P., Thomas, D. C. & Ward, D. C. Mutation detection and single-molecule counting using isothermal rolling-circle amplification. *Nat. Genet.* **19**, 225–232 (1998).
- [70] Baner, J., Nilsson, M., Mendel-Hartvig, M. & Landegren, U. Signal amplification of padlock probes by rolling circle replication. *Nucleic Acids Res.* **26**, 5073–5078 (1998).
- [71] Ali, M. M. & Li, Y. F. Colorimetric sensing by using allosteric-DNAzyme-coupled rolling circle amplification and a peptide nucleic acid-organic dye probe. *Angew. Chem., Int. Ed.* **48**, 3512–3515 (2009).
- [72] Li, J. S., Deng, T., Chu, X., Yang, R. H., Jiang, J. H., Shen, G. L. & Yu, R. Q. Rolling circle amplification combined with gold nanoparticle aggregates for highly sensitive identification of single-nucleotide polymorphisms. *Anal. Chem.* **82**, 2811–2816 (2010).
- [73] Cheglakov, Z., Weizmann, Y., Basnar, B. & Willner, I. Diagnosing viruses by the rolling circle amplified synthesis of DNAzymes. *Org. Biomol. Chem.* **5**, 223–225 (2007).
- [74] Nallur, G., Luo, C., Fang, L., Cooley, S., Dave, V., Lambert, J., Kukanskis, K., Kingsmore, S., Lasken, R. & Schweitzer, B. Signal amplification by rolling circle amplification on DNA microarrays. *Nucleic Acids Res.* **29**, e118 (2001).
- [75] Zhang, S., Wu, Z., Shen, G. & Yu, R. A label-free strategy for SNP detection with high fidelity and sensitivity based on ligation-rolling circle amplification and intercalating of methylene blue. *Biosens. Bioelectron.* **24**, 3201–3207 (2009).

- [76] Patolsky, F., Weizmann, Y. & Willner, I. Redox-active nucleic-acid replica for the amplified bioelectrocatalytic detection of viral DNA. *J. Am. Chem. Soc.* **124**, 770–772 (2002).
- [77] Nagamine, K., Hase, T. & Notomi, T. Accelerated reaction by loop-mediated isothermal amplification using loop primers. *Mol. Cell. Probes* **16**, 223–229 (2002).
- [78] Schaerli, Y., Stein, V., Spiering, M. M., Benkovic, S. J., Abell, C. & Hollfelder, F. Isothermal DNA amplification using the T4 replisome: Circular nicking endonuclease-dependent amplification and primase-based whole-genome amplification. *Nucleic Acids Res.* **38**, e201 (2010).
- [79] Ahmed, M. U., Saito, M., Hossain, M. M., Rao, S. R., Furui, S., Hino, A., Takamura, Y., Takagi, M. & Tamiya, E. Electrochemical genosensor for the rapid detection of GMO using loop-mediated isothermal amplification. *Analyst* **134**, 966–972 (2009).
- [80] Zhang, X., Qu, K., Li, Q., Cui, Z., Zhao, J. & Sun, X. Recording the reaction process of loop-mediated isothermal amplification (LAMP) by monitoring the voltammetric response of 2'-deoxyguanosine 5'-triphosphate. *Electroanalysis* **23**, 2438–2445 (2011).
- [81] Xuan, F., Luo, X. & Hsing, I. M. Sensitive immobilization-free electrochemical DNA sensor based on isothermal circular strand displacement polymerization reaction. *Biosens. Bioelectron.* **35**, 230–234 (2012).
- [82] Hsieh, K., Patterson, A. S., Ferguson, B. S., Plaxco, K. W. & Soh, H. T. Rapid, sensitive, and quantitative detection of pathogenic DNA at the point of care through microfluidic electrochemical quantitative loop-mediated isothermal amplification. *Angew. Chem., Int. Ed.* **124**, 4980–4984 (2012).

- [83] Erdem, A., Kerman, K., Meric, B., Akarca, U. S. & Ozsoz, M. Novel hybridization indicator methylene blue for the electrochemical detection of short DNA sequences related to the hepatitis B virus. *Anal. Chim. Acta* **422**, 139–149 (2000).
- [84] Yang, W., Ozsoz, M., Hibbert, D., Brynn & Gooding, J., Justin. Evidence for the direct interaction between methylene blue and guanine bases using DNA-modified carbon paste electrodes. *Electroanalysis* **14**, 1299–1302 (2002).
- [85] Kelley, S. O., Barton, J. K., Jackson, N. M. & Hill, M. G. Electrochemistry of methylene blue bound to a DNA-modified electrode. *Bioconjugate Chem.* **8**, 31–37 (1997).
- [86] Yang, L., Fung, C. W., Cho, E. J. & Ellington, A. D. Real-time rolling circle amplification for protein detection. *Anal. Chem.* **79**, 3320–3329 (2007).
- [87] Di Giusto, D. A., Wlassoff, W. A., Gooding, J. J., Messerle, B. A. & King, G. C. Proximity extension of circular DNA aptamers with real-time protein detection. *Nucleic Acids Res.* **33**, e64 (2005).
- [88] Ma, C., Wang, W., Yang, Q., Shi, C. & Cao, L. Cocaine detection via rolling circle amplification of short DNA strand separated by magnetic beads. *Biosens. Bioelectron.* **26**, 3309–3312 (2011).
- [89] Wu, Z.-S., Zhou, H., Zhang, S., Shen, G. & Yu, R. Electrochemical aptameric recognition system for a sensitive protein assay based on specific target binding-induced rolling circle amplification. *Anal. Chem.* **82**, 2282–2289 (2010).
- [90] Cheng, W., Yan, F., Ding, L., Ju, H. & Yin, Y. Cascade signal amplification strategy for subattomolar protein detection by rolling circle amplification and quantum dots tagging. *Anal. Chem.* **82**, 3337–3342 (2010).

- [91] Schweitzer, B., Wiltshire, S., Lambert, J., O'Malley, S., Kukanskis, K., Zhu, Z., Kingsmore, S. F., Lizardi, P. M. & Ward, D. C. Immunoassays with rolling circle DNA amplification: A versatile platform for ultrasensitive antigen detection. *Proc. Natl. Acad. Sci. U. S. A.* **97**, 10113–10119 (2000).
- [92] Ellington, A. D. & Szostak, J. W. In vitro selection of RNA molecules that bind specific ligands. *Nature* **346**, 818–822 (1990).
- [93] Tuerk, C. & Gold, L. Systematic evolution of ligands by exponential enrichment: RNA ligands to bacteriophage T4 DNA polymerase. *Science* **249**, 505–510 (1990).